Energetic and Exergetic Analyses of a Direct Steam Generation Solar Thermal Power Plant in Cyprus

Armita Hamidi

Submitted to the
Institute of Graduate Studies and Research
in partial fulfillment of the requirements for the Degree of

Master of Science
in
Mechanical Engineering

Eastern Mediterranean University
August 2012
Gazimağusa, North Cyprus

Approval of the Institute of Graduate Studies and Research

Prof. Dr. Elvan Yılmaz
Director

I certify that this thesis satisfies the requirements as a thesis for the degree of Master of Science in Mechanical Engineering.

Assoc. Prof. Dr. Uğur Atikol
Chair, Department of Mechanical Engineering

We certify that we have read this thesis and that in our opinion it is fully adequate in scope and quality as a thesis for the degree of Master of Science in Mechanical Engineering.

Assoc. Prof. Dr. Uğur Atikol
Supervisor

Examining Committee

1. Assoc. Prof. Dr. Fuat Egelioğlu _____

2. Assoc. Prof. Dr. Uğur Atikol _____

3. Asst. Prof. Dr. Hasan Hacışevki _____

ABSTRACT

In recent decades, the threat of climate change and other environmental impacts of fossil fuels have reinforced interests in alternative and renewable energy sources for producing electricity. In this regard, solar thermal energy can be utilized in existing power generation plants as replacement for the heat produced by means of fossil fuels.

The objective of this study is to investigate the energetic and exergetic feasibility of utilizing a solar thermal power plant in Cyprus. The analysis carried out is two-fold. First, the efficiency of each component of an existing steam power plant (Teknecik) is estimated using energy and exergy analyses. The results show that the boiler of this power plant has the highest irreversibility rate due to the combustion process of Fuel oil No.6 that happens in the boiler. In the second step, it is proposed to change the conventional power plant into a direct steam generation solar power plant. In this regard, parabolic trough collectors are used to generate superheated steam at 87 bars and 510˚C. Moreover, the energy and exergetic efficiency of each component of the new design has been estimated and compared with the results that obtained in the first part.

The highest exergy losses occurred in the collectors while the receiver subsystem has the maximum energy losses. Furthermore, the average exergy efficiency of the solar field is 24% while the boiler average exergy efficiency is 50%. The outcome clarifies that a DSG power plant has poor energetic and exergetic feasibility due to the high rate of losses. Nevertheless, the exergy analysis shows the cause and the location of

the losses which are worthwhile for optimizing and improving the solar field design. This can make the solar thermal power generation competitive with current technologies for producing electricity in large scales.

Keywords: energy, exergy, steam power plant, solar thermal power plant, direct steam generation

ÖZ

Son yıllarda iklim değişikliği tehdidi ve diğer çevresel etkiler yüzünden elektrik üretimi için alternatif ve yenilenebilir enerji kaynaklarına olan ilgi giderek artmıştır. Bu çerçevede, mevcut santrallerde fosil yakıt kullanılarak elde edilen ısı yerine güneş enerjisi kullanılabilmektedir.

Bu çalışmanın amacı Kıbrıs'ta güneş enerjisiyle çalışacak bir santralin enerjik ve ekserjetik fizibilitesini araştırmaktır. Çalışmada bu konuda yapılan analiz iki bölümden oluşmaktadır. İlk olarak, enerji ve ekserji analizleri kullanılarak Teknecik'teki mevcut buhar santralinin ayrı ayrı tüm kısımlarının verimliliği saptanmıştır. Sonuçlar bize göstermiştir ki santralda, en yüksek tersınmezlik oranına (6 numaralı fuel-oil yakıtının yanma sürecinden dolayı) buhar kazanında. İkinci olarak, klasik enerji santrali yerine doğrudan buhar üreten güneş santralinin kullanılması önerilmektedir. Bunun için parabolik oluk kollektörleri kullanılarak 87 bar ve 510 santigrat derecelik kızgın buhar meydana getirilmesi gerekmektedir. Ayrıca, yeni tasarımdaki tüm kısımların enerji ve ekserji verimliliği saptanmış ve bunlar ilk kısımda elde edilen sonuçlarla kıyaslanmıştır.

En büyük ekserji kayıpları kollektörlerde meydana gelirken maksimum kayıp alıcı altsisteminde gerçekleşmiştir. Ayrıca, güneş tarlasındaki ortalama ekserji verimliliği %24 olurken, kazandaki ortalama ekserji verimliliği %50 olarak gerçekleşmiştir. Bu sonuca göre, yüksek düzeydeki kayıplardan dolayı doğrudan buhar üreten (DSG) bir santralin enerji ve ekserji fizibiliteleri düşüktür. Yine de ekserji analizi bu kayıpların sebebini ve konumunu gösterdiği için güneş tarlası tasarımını optimize etmeye ve

geliştirmeye yaramaktadır. Bu da büyük çaplarda elektrik üretimlerinde, güneş enerjisi sistemlerini mevcut teknolojilerle şimdikinden daha rekabet edebilir hale getirebilir.

Anahtar Kelimeler: Enerji, ekserji, buhar santrali, güneş enerjisi santrali, doğrudan buhar üretimi.

Dedicated to

the memory of my beloved grandfather

ACKNOWLEDGEMENT

It would not have been possible to write this master thesis without the help and support of the kind people around me, to only some of whom it is possible to give particular mention here.

First and foremost I offer my sincerest gratitude to my supervisor and Head of the Mechanical Engineering Department, Assoc. Prof. Dr. Uğur Atikol, who has supported me throughout my thesis with his patience and knowledge whilst allowing me the room to work in my own way. I attribute the level of my Master's degree to his encouragement and effort and without him this thesis, too, would not have been completed or written. One simply could not wish for a better or friendlier supervisor.

I would like my sister, Dr. Anahita Hamidi who supported and assisted me in writing and editing my work.

I also would like to thank all of my colleagues and staff at Mechanical Engineering Department for their technical and moral support. Likewise all of my kind friends in Cyprus.

Last, but by no means least, I thank my wonderful parents, who always support and encourage me to achieve success.

TABLE OF CONTENTS

LIST OF TABLES

LIST OF FIGURES

NOMENCLATURE

A_a	Absorber Area (m2)
A_r	Receiver Area (m2)
B	Aperture Width (m)
C	Concentration Ratio
C_p	Specific Heat (kJ/kg.K)
D_o	Receiver Outside Diameter (m)
D_i	Receiver Inside Diameter (m)
D_{ci}	Glass Cover Inside Diameter (m)
D_{co}	Glass Cover Outside Diameter (m)
$\dot{Ex}$	Exergy rate (kW)
g	Gravitational Acceleration
I_b	Solar Beam radiation (DNI) (W/m2)
$\dot{IR}$	Destroyed Irreversibility (kW)
K_c	Thermal Conductivity of Glass Cover (W/m K)
h	Enthalpy(kJ/kg)
L	Length of the Collector (m)
$\dot{m}$	Mass Flow Rate (kg/s)
N_c	Number of collectors
N_r	Number of rows
$\dot{Q}$	Heat Transfer Rate (kW)
Q_I	Solar power input to parabolic trough (kW)
Q_a	Solar power absorbed by receiver/absorber (kW)
Q_u	Useful thermal power gain by thermic fluid (kW)

R_b	Tilt Factor
s	Entropy(kJ/kg.K)
T_s	Sun Temperature (K)
T_r	Receiver Temperature (K)
T_a	Ambient Temperature (K)
U_l	Loss Coefficient of the Solar Field (W/m2.K)
$\dot{W}$	Work Rate (kW)
w	Width of the Parabolic Trough Collector (m)
V	Velocity (m/s)
Z	Elevation (m)

SYMBOLS

α	Absorptivity
δ	Declination (º)
ε_c	Emissivity of Glass
ε_r	Emissivity of the Receiver
θ	Angle of Incidence (º)
θ_z	Zenith Angle (º)
η_o	Optical efficiency
η_I	Energy Efficiency
η_{Π}	Exergy Efficiency
σ	Stefan's Constant
ψ	Specific Exergy (kJ/kg)
φ	Latitude (º)
ω	Hour angle (º)

ABBREVIATION

BFP	Boiler feed water pumps
CSP	Concentrated Solar Power
CFP	Condensate Feedwater pump
DNI	Direct Normal Irradiation
EES	Engineering Equation Solver
HHV	Higher Heating Value
HPH	High Pressure Feedwater Heater
LHV	Lower Heating Value
LPH	Low Pressure Feedwater Heaters
PTC	Parabolic Trough Concentrator
STPP	Solar thermal power plant
PTCSTPP	Parabolic Trough Concentrating Solar Thermal Power Plant

Chapter 1

INTRODUCTION

As the price of carbon fuels increase and as the cost of pollution is factored into conventional generation, it is expected that renewable energy sources become more viable. Exploiting solar energy for producing power is one of options which has already shown an enormous promise. Solar power is generating electricity from solar energy, either directly using photovoltaics (PV), or indirectly using concentrated solar power (CSP). The benefits of solar power which are compelling as environmental protection, economic growth, job creation and diversity of fuel supply, make it a prime choice in developing an affordable, feasible and global energy source that is able to substitute for fossil fuels in the sunbelt countries around the world.

1.1 The Case of Cyprus

Cyprus as an island in Mediterranean region has no natural hydrocarbon energy sources. Electricity production in Cyprus is almost completely relied on imported fuels such as, heavy fuel oil and diesel with a share of 98% and 2% respectively [1]. Geographically Cyprus is located on a sun belt with an average yearly 1790 kWh/m² solar radiation receiving on the flat surface [1]. A considerable high sunlight radiation is received from April to September which is one of the ideal situations for installing a parabolic trough solar thermal technology for electricity generation. All parts of Cyprus receive a plentiful of solar energy. The island is to be exposed to sunlight radiation on average 9.8 hours in December to 14.5 hours in June [1]. Solar

energy is used only for heating water in about 90% houses and apartments and 50% of hotels. This makes Cyprus the first country around the world with installed solar collector per inhabitant [2].

1.2 Solar Thermal Power Plants

Solar thermal power uses direct sunlight, so it must be sited in regions with high direct solar radiation such as South-Western United States, Central and South America, North and Southern Africa, the Mediterranean countries of Europe, the Middle East, Iran, the desert plains of India, Pakistan, the former Soviet Union, China and Australia. Worldwide experience shows that, setting up solar thermal technology in one square kilometer of land is enough to generate approximately 110 gigawatt hours (GWh) of electricity per year which is comparable to the annual production of a 50 MW fossil-fired mid-load power unit [3].

Growing demand of power which resulted in the degradation of the environment has placed the solar power plants on the agenda for clean power production. Advanced technologies, mass production, economies of scale and improved operation will together enable a reduction in the cost of solar electricity to a level competitive with fossil-fueled power stations within the next 10 to 15 years [4]. Since solar thermal power plants (STPP) is spreading widely nowadays, there are numbers of different technologies which have been produced recently for performing of kind of power. However, there is still room for improving the design and performance.

Producing electricity from the solar thermal energy is a straightforward process: direct solar radiation can be concentrated and collected by a range of Concentrating Solar Power (CSP) technologies to provide medium to high temperature heat. This

heat is then used to operate a conventional power cycle, for example through a steam turbine or a Stirling engine. Solar heat collected during the day can also be stored in liquid or solid media like molten salts, ceramics, concrete or, in the future, phase-changing salt mixtures. At night, it can be extracted from the storage medium and, thus, continues turbine operation. In direct steam generation technology which send the high temperature steam directly to the power cycle, there is no need of a heat exchanger between the solar field and the power block and so there is no additional heat losses and pressure drops in the global efficiency.

1.3 Objectives

The aim of this study is to utilize the energy and exergy techniques to evaluate the feasibility of converting the conventional power plant in Cyprus into a solar thermal power plant. Since the parabolic trough mirrors are proven all over the world, the study will consider this technology as the heating medium for the working fluid. The design of the solar field in this study will be based on direct solar thermal technology which there is no heat exchanger and therefore, no additional loss is produced.

Solar radiation and ambient temperature are two important factors in designing the solar field [5]. They have direct effect on the performance of the solar thermal power plants. Therefore, studying the performance of the components and the whole plant with varying these two parameters will help to provide further achievement in designing and optimizing the solar thermal power technology.

1.4 Organization of the Thesis

The structure of this research is organized as follows: Chapter 2 includes a review about the history of solar thermal power plants and energy and exergy analyses for solar systems. Chapter 3 includes the equations which is useful for exergy analysis

for solar system and Rankine cycle. The results of exergy analysis of the steam power plant are reported in chapter 4. The design of the solar field which is installed instead of boiler is described in chapter 5. Moreover, the results of energy and exergy analysis of the collector-receiver system are presented in this chapter. The last chapter is discussed about the components which have the lower exergy efficiency. Additionally this thesis includes multiple diagrams comparing the results before and after solar field installation. Based on our findings, the components which have the lower exergy efficiency will be discussed in the last chapter of this thesis in addition to recommendation for optimizing the whole system and its components which can hopefully be practical in near future.

Chapter 2

LITERATURE REVIEW

Producing electricity at central power stations has been begun since 1881. In primary power plants water power or coal were used. In 2008, 67% of the electricity produced around the world is based on fossil fuels (coal, oil and gas) [12]. Most steam power plants burn fossil fuels for producing superheated steam to drive large steam turbines which are coupled with an electrical generator to produce power. But the sources of fossil fuels are finite. Moreover, burning such kinds of fuels release large scales of carbon dioxide into atmosphere enhancing the greenhouse effect and contributing to global warming. The estimated CO_2 emission from the world's electrical power industry is 10 billion tons per year [7]. Therefore, efforts to provide sufficient alternative energy sources without limitation of utilization and lower environmental and climatic hazards have been made and recently renewable energy become more popular. Renewable energy utilization grew from 10% to 60% per year for many technologies in the world since 2004 [8].

The first commercial concentrated solar power plants were developed in the 1980s. The largest solar power plant in the world is located in the Mojave Desert of California which has the capacity of 354 MW of electricity. Nowadays installation and utilization of these kinds of power plants is spreading widely among the countries which placed on the sun-belt. Four different types of solar technology

mainly used in concentrating solar power plants: parabolic trough, power tower, dish/engine and linear Fresnel reflectors.

Among these available options, parabolic trough collectors is the most promising and further advanced than others. This technology is used at Nevada solar plant in the United States [9] and at the Andasol plants in Spain [10]. According to the 'Global Concentrated Solar Power Industry' report 2010–2011, parabolic trough technology is the most developed CSP technology with around 90% of total currently operating plants (more than 500MW) in the world [11].

The design of the parabolic trough solar thermal power plant which is evaluated in this research is based on the Direct Steam Generation (DSG). The other alternatives require a Heat Transfer Fluid (HTF) and a Heat Recovery Steam Generator (HRSG) between the solar field and the power block, which produces additional heat losses. Although DSG can be said to be a new technology, it is a highly promising option to increase the efficiency of the whole system. The feasibility of the DSG process in horizontal parabolic trough collectors has already been proven in the DISS project [12]. DISS was a complete program with two phases during January 1996 to August 2001 with the aim of developing DSG technology using parabolic trough collectors. The objective of this project was reducing costs while increasing the efficiency.

The design of the first precommercial DSG solar power plant was applied in the INDITEP project, which is promoted by a Spanish-German consortium of engineering companies, power equipment manufacturers, research centers and businesses involved in the energy market such as Iberdrola Ingenierı´a Consultorı´a (Project Coordinator), CIEMAT, DLR, FLAGSOL GmbH, FRAMATONE,

GAMESA Energı´a Servicios S.A., INITEC Tecnologı´a S.A., Instalaciones Inabensa S.A. and ZSW. In 2009, Montes analyze the performance of a 50 MW DSG power plant for electricity production as a function of the solar multiple. At present, there are two projects to develop pre-commercial demonstration plants based on DSG technology, they all to be implemented in the southern of Spain. Net electrical power of these plants will be 3MWe [13] and 5MWe [14], respectively.

Generally, the evaluation of the thermal power plant performance is through the energy analysis based on the first law of thermodynamics which can demonstrate the electrical power and thermal efficiency. "In recent decades, the exergetic performance based on the second law of thermodynamics was found to be useful in the design, evaluation, optimization and improvement of thermal power plants" [15]. Kotas [16] published a full description about the exergy method in his book. In 2001, Dincer [17] analyzed a Rankine cycle reheat steam power plant to study the energy and exergy efficiencies at different operating conditions with varying boiler temperature, boiler pressure, mass fraction ratio and work output from the cycle. Since then several studies have been done on different kinds of power plants by different scientists such as Fischer [18], Ameri [19], Cihan [20], Habib [21] and Rosen [22]. While developing and replacing alternative energy sources, the goal of efficient use of these kinds of energy resources is also promoted. In this regard, Singh [23-24] and Bannister [25-26] in their papers on high temperature solar thermal power collector systems, presented simple models for solar thermal power collector systems based on the exergy concept in order to evaluate the thermodynamic losses. However, their methods are complicated and not easy to follow and hence, could not be further developed for other systems. Later, in 2000, Singh [27] added the second law analysis (based on the exergy concept) to a solar

thermal power system using a parabolic trough collector system which connected to a Rankine heat engine cycle for power generation to evaluate the actual available exergy and second law efficiency. More recently, Gupta and Kaushik [28] performed exergy analysis for 5 MW DSG power plant with various feed water heaters in order to minimize the exergy losses and improving the efficiency.

The novelty of the present study is that, a new design of a system using DSG technology with parabolic solar trough collectors has been proposed for a system to produce 50 MW which can be considered as a high power capacity plant. For studying and optimizing the solar field design the energy and exergy analysis (based on first and second law of thermodynamics respectively) is to be carried out in order to pinpoint the location and magnitude of the process irreversibilities leading to optimization of the system.

Chapter 3

METHODOLOGY

3.1 Energy and Exergy Analyses

One of the most powerful tools is widely used in the design, simulation and performance evaluation of any energy systems is the exergy analysis (or the second law analysis). Energy analysis which is based on the first law of thermodynamics gives only the quantitive assessment of the various losses occurring in the components of any system. On the other hand, exergy analysis method is employed to detect and evaluate quantitatively the causes of the thermodynamic imperfections and it is able to indicate the possibilities of thermodynamic improvements of the process under consideration. Considering both the energetic and exergetic performance criteria together can guide the ways of efficient and effective usage of fuel resources by taking into account the quality and quantity of the energy used in the generation of electric power in thermal power plants [15].

The first law of thermodynamics or energy balance for the steady flow process of an open system is given by:

$$\sum \dot{Q}_K + \sum_{in} \dot{m}\left(h + \frac{V^2}{2} + gZ\right) = \sum_{out} \dot{m}\left(h + \frac{V^2}{2} + gZ\right) + \dot{W} \qquad (3\text{-}1)$$

Where $\dot{Q}_K$ is the heat transfer to system from source at T_K and W is the net work. The energy of the flowing fluid per unit mass is $h + \frac{V^2}{2} + gZ$ where h is the enthalpy (representing internal energy), V is the velocity of the flow (representing kinetic

energy) and Z is the elevation of the system relative to some external reference point. The mass flow rate of the fluid is $\dot{m}$ and g is the gravitational acceleration.

The energetic efficiency of system is defined as:

$$\eta_I = \frac{\text{Desired Output Power}}{\text{Input Power Supplied}} \tag{3-2}$$

"Exergy is defined as the maximum amount of work which can be produced by a stream of matter, heat or work as it comes to equilibrium with a reference environment" [29]. "The exergy of heat transfer from the control surface at temperature T is determined from maximum rate of conversion of thermal energy to work W_{max}" [28]:

$$W_{max} = Ex^Q = Q\left(1 - {}^{T_0}/_{T}\right) \tag{3-3}$$

T_0 is the ambient temperature.

The exergy flow for steady flow process of an open system is given by:

$$\sum(1 - \tfrac{T_0}{T_k})\dot{Q}_k + \sum_{in} \dot{m}\,\psi = \dot{m}\psi_w + \sum_{out} \dot{m}\,\psi + \dot{I}_{destroyed} \tag{3-4}$$

Where exergy ψ is expressed as:

$$\psi = [(h^0 - h_o^0) - T_0(s - s_0)] \tag{3-5}$$

h^0 denotes the total energy in the system which is:

$$h^0 = h + \frac{V^2}{2} + gZ \tag{3-6}$$

The exergy destroyed is proportional to the entropy generated [36]:

$$\dot{I}_{destroyed} = T_0\dot{S}_{gen} \tag{3-7}$$

The exergy or second law efficiency is defined as:

$$\eta_{II} = \frac{Actual\ Thermal\ Efficiency}{Maximum\ Possible(reversible) Thermal efficiency} = \frac{Exergy\ Output}{Exergy\ Input} \tag{3-8}$$

3.2 Analysis of the Components of the Power plant

Exergy analysis measures the maximum capacity of a system to perform useful work as it proceeds to a specified final state in equilibrium with its surroundings which is called dead state. Unlike energy, exergy is not conserved but it is destructed in the system. Exergy destruction is equivalent to the irreversibilities which are the sources of the performance losses. Therefore, an exergy analysis assessing the magnitude of exergy destruction identifies the location, the magnitude and the source of thermodynamic inefficiencies in a thermal system. It is possible to perform an exergy analysis for each component of the Teknecik steam power plant to determine its exergetic efficiency. This is usually done so by ignoring the kinetic and potential energy changes in the equations, and assuming steady state operation.

Figure 3-1 shows the thermodynamic cycle of the Teknecik power plant. The cycle consists of a boiler, a turbine, a condenser, two pumps and five feed water steam and DSG design of the power plant. The main fuel of the boiler is Fuel oil No.6. Turbine which is coupled with the generator has the capacity to produce 60 MW of electricity at the full load state. The cooling water of condenser is directly supplied from the sea since installation of cooling tower is not possible because of the high relative humidity of the air in the power plant site. The task of the pump which installing after the condenser is providing the condensate water with the pressure of 13 bars for the first low pressure feedwater heater. The mentioned cycle has two low pressure and two high pressure feed water heater and a deaerator. The water which exits the deaerator is pumped to the first high pressure feed water heater by the boiler feed water pump.

It is desired to replace the boiler by the solar thermal collectors to convert the system into a solar thermal power plant. The solar thermal power system can be divided into two subsystems, namely, the collector-receiver and the Rankine cycle subsystems which is the common part with the conventional steam power plant.

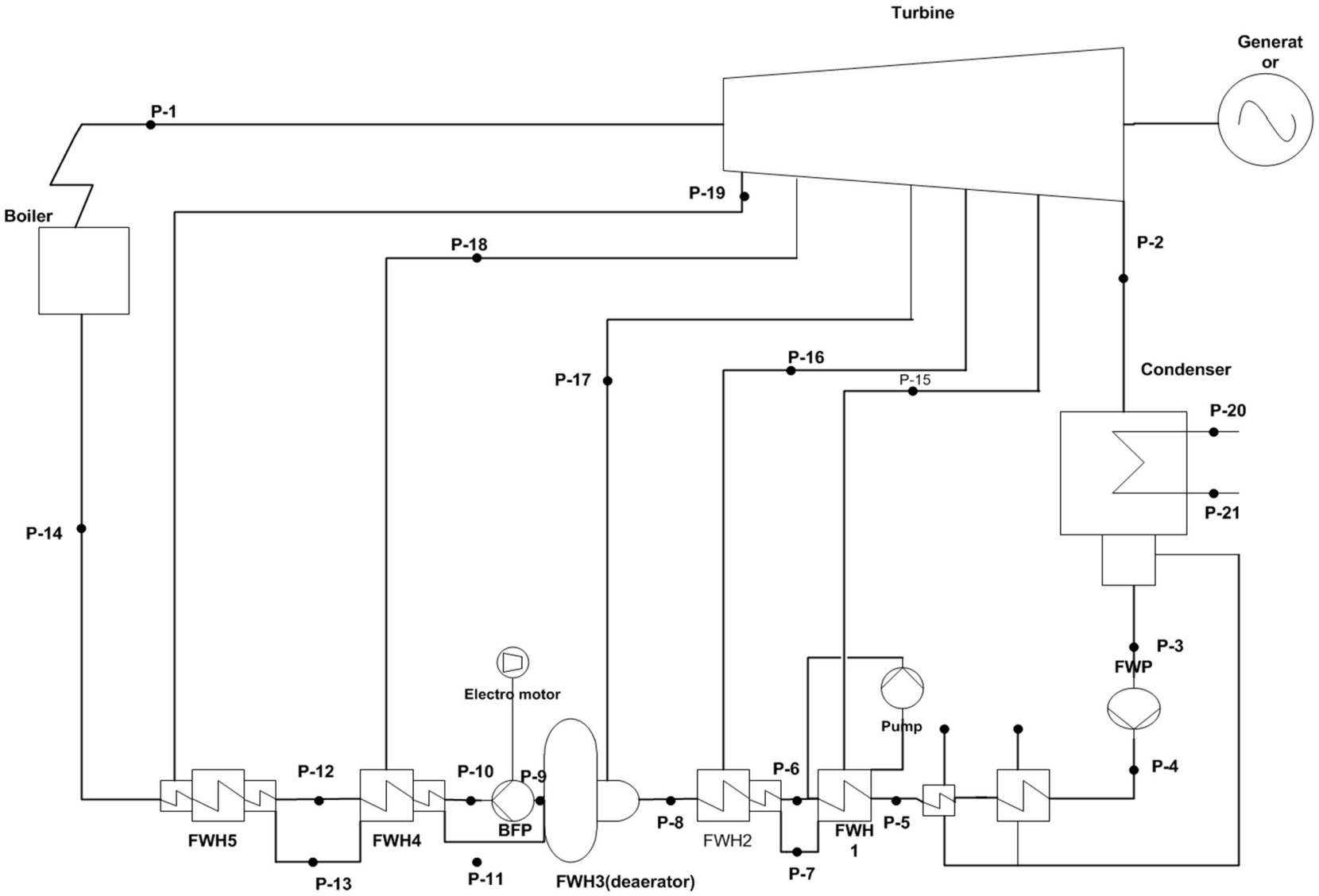

Fig.3- 1. Fossil fuel fired 60 MW steam cycle power plant

3.2.1 Solar Field

The solar field consists of a number of parabolic trough collectors arranged in modules operating in tracking mode. The parabolic trough mirrors are divided into two subsystems, namely the collector and the receiver.

3.2.1.1 Collector Subsystem:

Energy received by the collector system is:

$$Q_I = I_b R_b B L N_c N_r \tag{3-9}$$

where B is the width of the aperture of the collector, I_b is the beam radiation falling on horizontal surface, R_b is the tilt factor, N_c is the number of collector rows and N_r is the number of collectors in each row. The tilt factor is calculated by:

$$R_b = cos\theta / cos\theta_z \tag{3-10}$$

θ is the angle between the beam radiation on a surface and the normal to that surface which is called the angle of incidence and θ_z is zenith angle which is between the vertical axis and the line to the sun, i.e., the angle of incidence of beam radiation on horizontal surface [30].

$$\cos\theta = [(\sin\varphi \sin\delta + \cos\varphi \cos\delta \cos\omega)^2 + cos^2\delta sin^2\omega]^{1/2} \tag{3-11}$$

$$\cos\theta_z = \sin\varphi \sin\delta + \cos\varphi \cos\delta \cos\omega \tag{3-12}$$

Declination δ is the angular position of the sun at solar noon (i.e., when the sun is on the local meridian) with respect to the plane of the equator, north positive [30];

$$-23.45° \leq \delta \leq 23.45° \tag{3-13}$$

$$\delta = 23.45 \sin(360(284 + n)/365) \tag{3-14}$$

n is the number of day in the year.

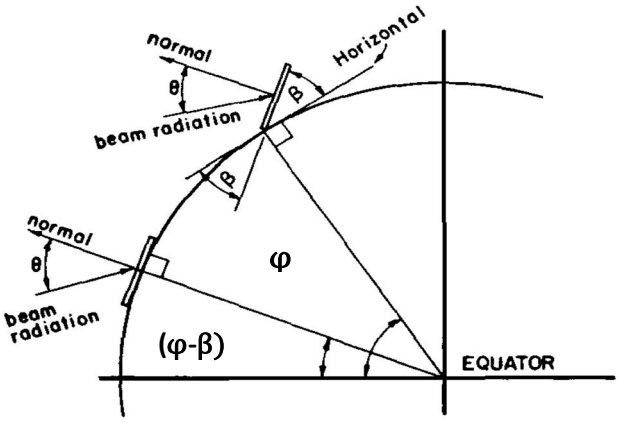

Figure 3-2. Section of Earth Showing θ for a South Facing Surface [30]

" φ is the latitude and ω is the hour angle which is the angular displacement of the sun east or west of the local meridian due to the rotation of the earth on its axis at 15º per hour, morning negative, afternoon positive" [30].

The total exergy received by the collector system is computed by:

$$Ex_I = Q_I[1 - \frac{4}{3}\left(\frac{T_a}{T_s}\right) + \frac{1}{3}\left(\frac{T_a}{T_s}\right)^4] \quad (3\text{-}15)$$

T_a is the ambient temperature and T_s is apparent black body temperature of the sun which is approximately 5600K.

3.2.1.2 Receiver Subsystem:

The energy and exergy which is absorbed by the receiver/absorber of solar collector field is as following:

$$Q_a = \eta_o I_b R_b B L N_c N_r \quad (3\text{-}16)$$

Where η_o is the optical efficiency at the design point.

$$Ex_a = Q_a(1 - {}^{T_a}/_{T_r}) \quad (3\text{-}17)$$

In equation (3-17) T_r is the mean temperature of the absorber.

$$Q_l = U_l \pi D_o (T_r - T_a) L \quad (3\text{-}18)$$

Q_l is the heat loss from the collector which Takes place in the absorber. For reducing the heat loss, absorber tube is enveloped with vacuum glass tube. Depending on the thermal resistances between the absorber tube surface and the surroundings, the heat loss coefficient U_l is calculated iteratively [30] by solving the following equations [31-33]:

$$\acute{q}_{loss} = U_l \pi D_o (T_r - T_a) \tag{3-19}$$

$$\acute{q}_{loss} = \acute{q}_{co-s} = \pi D_{co} h_w (T_{co} - T_a) + \varepsilon_c \pi D_{co} \sigma (T_{co}^4 - T_s^4) \tag{3-20}$$

$$\acute{q}_{loss} = \acute{q}_{ci-s} = 2\pi k_c (T_{ci} - T_{co}) / ln(D_{co}/D_{ci}) \tag{3-21}$$

$$\acute{q}_{loss} = \acute{q}_{r-ci} = \pi D_o \sigma (T_r^4 - T_{ci}^4) / [\frac{1}{\varepsilon_r} + \frac{D_o}{D_{ci}} \left(\frac{1}{\varepsilon_c} - 1\right)] \tag{3-22}$$

h_w is wind heat transfer coefficient and ε_c is the emissivity of glass cover. $\acute{q}_{co-s}$ and $\acute{q}_{ci-s}$ is the heat loss from the outer and inner surface of the glass cover of receiver to the surroundings and $\acute{q}_{r-ci}$ is the heat loss from the surface of the steel tube of receiver. The emissivity ε_r of the coating of receiver in terms of T_r is taken equal to [34]:

$$\varepsilon_r = 0.00042 T_r - 0.0995 \tag{3-23}$$

The correlation for U_l in terms of T_r is obtained as [28]:

$$U_l = 9.64479 - 0.0429686 T_r + 0.0000541032 {T_r}^2 \tag{3-24}$$

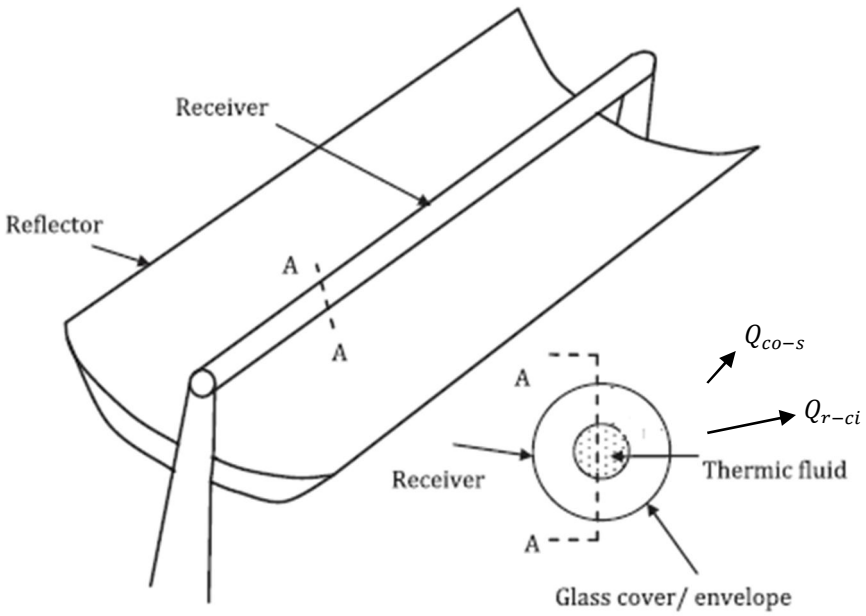

Figure 3-3. Parabolic Trough Collector [38]

The useful heat which is transferred to water flowing through receiver tube is calculated by:

$$Q_u = m_{collector,out} h_{collector,out} - m_{collector,in} h_{collectorin} \quad (3\text{-}25)$$

The useful exergy is given by:

$$Ex_u = m_{collector.out} \psi_{collector.out} - m_{collector,in} \psi_{collector,in} \quad (3\text{-}26)$$

3.2.2 Steam Power Cycle

The thermodynamic analysis of components related to the Rankine cycle of the power plant is carried out based on the following equations:

$Continuity\ equation$:

$$\sum \dot{m}_{in} = \sum \dot{m}_{out} \quad (3\text{-}27)$$

$Energy\ equation$:

$$\dot{Q} - \dot{W} = \sum \dot{m}_{out}\, h_{out} - \sum \dot{m}_{in}\, h_{in} \quad (3\text{-}28)$$

$Exergy\ balance\ equation$:

$$\dot{Ex}_Q + \sum \dot{m}_{in}\,\psi_{in} = \sum \dot{m}_{out}\,\psi_{out} + \dot{Ex}_W + \dot{Ex}_D + \dot{Ex}_L \quad (3\text{-}29)$$

3.2.2.1 Boiler:

The combustion process in the boiler is the main reason of losses and irreversibilities i.e., exergy destruction. For the evaluation of the fuel exergy, ξ which is the corresponding ratio of simplified exergy is defined as the following:

$$\xi = \psi_f / LHV_f \quad (3\text{-}30)$$

For gaseous fuel with C_xH_y, the following empirical equation is used to calculate ξ [35]:

$$\xi = 1.033 + 1.0169\frac{y}{x} - \frac{0.0698}{x} \quad (3\text{-}31)$$

The exergy analysis for the boiler of the steam power plant [Fig. 3-1] is carried out as follows:

$$\dot{Ex}_{in,b} = \dot{Ex}_{14} + \dot{Ex}_{air} \quad (3\text{-}32)$$

In the following equations Ex_j at state point j is represented the exergy of that point.

$$\dot{Ex}_{out,b} = \dot{Ex}_1 + \dot{Ex}_{exhaust} \quad (3\text{-}33)$$

$\dot{Ex}_{exhaust}$ is related to the mixture of gases flows throughout the chimney of the power plant. The chemical exergy of a mixture is calculated by:

$$\dot{Ex}_{exhaust} = \sum_i x_i \bar{\varepsilon}_{0,i} + \bar{R}T_a \sum_i x_i Ln x_i \quad (3\text{-}34)$$

x_i is the molar percentage of each component of the mixture and $\bar{\varepsilon}_{0,i}$ is the molar specific exergy of that component.

The irreversibility rate and exergy efficiency is defined:

$$\dot{IR}_b = \dot{Ex}_f + \dot{Ex}_{in,b} - \dot{Ex}_{out,b} \quad (3\text{-}35)$$

$$\eta_{\Pi,b} = \frac{\dot{Ex}_{in,b} - \dot{Ex}_{out,b}}{\dot{Ex}_f} = 1 - \frac{\dot{IR}_b}{\dot{Ex}_f} \quad (3\text{-}36)$$

3.2.2.2 Turbine:

The exergy analysis for the turbine is as follows:

$$\dot{E}x_{in,t} = \dot{E}x_1 \tag{3-37}$$

$$\dot{E}x_{out,t} = \dot{E}x_2 + \dot{E}x_{15} + \dot{E}x_{16} + \dot{E}x_{17} + \dot{E}x_{18} + \dot{E}x_{19} \tag{3-38}$$

$$I\dot{R}_t = \dot{E}x_{in,t} - \dot{E}x_{out,t} - \dot{W}_t \tag{3-39}$$

$$\eta_{\Pi,t} = \frac{\dot{W}_t}{\dot{E}x_{in,t} - \dot{E}x_{out,t}} \tag{3-40}$$

3.2.2.3 Condenser:

Exergy balance related to the condenser is calculated:

$$\dot{E}x_{in,c} = \dot{E}x_2 + \dot{E}x_{20} \tag{3-41}$$

$$\dot{E}x_{out,c} = \dot{E}x_3 + \dot{E}x_{21} \tag{3-42}$$

$$I\dot{R}_c = \dot{E}x_{in,c} - \dot{E}x_{out,c} \tag{3-43}$$

$$\eta_{\Pi,c} = \frac{\dot{E}x_{out,c}}{\dot{E}x_{in,c}} \tag{3-44}$$

3.2.2.4 Pump:

The exergy destruction and exergy efficiency of the pump is:

$$I\dot{R}_p = \dot{E}x_{in,p} - \dot{E}x_{out,p} + \dot{W}_p \tag{3-45}$$

$$\eta_{\Pi,p} = \frac{\dot{E}x_{in,t} - \dot{E}x_{out,p}}{\dot{W}_p} \tag{3-46}$$

3.2.2.5 Feed Water Heater:

For feed water heater which is a heat exchanger, the equations are similar to the condenser:

$$I\dot{R}_h = \dot{E}x_{in,h} - \dot{E}x_{out,h} \tag{3-47}$$

$$\eta_{\Pi,h} = \frac{\dot{E}x_{out,h}}{\dot{E}x_{in,h}} \tag{3-48}$$

3.2.3 Whole Power Plant:

The energy and exergy efficiency of the whole plant is calculated by:

$$\eta_I = \frac{W_t - W_p}{Q_I} \tag{3-49}$$

$$\eta_{II} = \frac{W_t - W_p}{Ex_I} \tag{3-50}$$

Chapter 4

ENERGETIC AND EXERGETIC ANALYSES OF THE EXISTING STEAM POWER PLANT

4.1 System Description of the Steam Power Plant

Teknecik power plant has two steam units each having installed capacity of 60 MW. The cycle consists of a boiler, a turbine with five extraction lines for feed water heaters, a condenser, a condensate extraction pump, a boiler feed water pump, two high pressure feed water heater, a deaerator and two low pressure feed water heater as shown in Figure 3-1. The present study considers one power unit and assumes that it is operating with almost 83% full load (50 MW). The boiler consumes 15 tons/ hour of fuel oil No.6 for producing 50 MWh power. Table 4-1 shows the thermodynamic properties of each point of the steam power cycle (defined in Figure 3-1).The steam enters the turbine at 510ºC. Cooling water enters the condenser at 28.5ºC and mass rate of 2305 kg/s. The analysis has been performed for a day in each month during a year in order to observe the results for different seasons and temperatures.

Table 4-1.Stream data of steam power cycle

Point*	$\dot{m}$ (kg/s)	T(°C)	P(bar)	h(kJ/kg)	s(kJ/kg.K)
P-1	63	510	87	3415.1	6.709
P-2	41.892	40.81	0.077	2262.57	7.246
P-3	44.968	40.81	0.07706	170.95	0.5831
P-4	44.996	41.22	13	173.67	0.588
P-5	44.996	42.81	13	180.34	0.6091
P-6	50.511	69.41	13	291.54	0.947
P-7	3.323	84.41	13	353.5	1.127
P-8	50.511	104	13	436.81	1.351
P-9	63	136.61	3.28	574.51	1.704
P-10	63	138.22	105	588.2	1.711
P-11	9.695	148.22	0.0045	624.77	1.8231
P-12	63	174.23	105	742.9	2.071
P-13	5.802	184.23	0.001	782.47	2.1805
P-14	63	222	105	955.23	2.524
P-15	1.922	73.72	0.365	2410.89	7.062
P-16	3.323	108.89	1.38	2575.19	6.952
P-17	1.31	139.52	3.565	2718.82	6.9
P-18	6.463	234.26	9.9	2907.93	6.861
P-19	6.252	338.54	24.89	3102.06	6.799
P-20	2430	28.5	0.03229	119.52	0.416
P-21	2430	37.57	0.0653	157.4175	0.5398

*Points are shown on the steam power cycle in Fig. 3-1.

Table 4-2. Fuel Properties and components

Fuel type	fuel oil No.6
Lower heating value (LHV)	41 MJ/kg
Higher heating value (HHV)	43 MJ/kg
Fuel mass flow rate	15 ton/hour
Fuel exergy	42.078 MJ/kg
Carbon	87.87%(molar mass)
Hydrogen	10.33%
Sulphur	1.16%
Nitrogen	0.14%
Oxygen	0.5%

4.2 Energy and Exergy Analysis results

4.2.1 Boiler:

In North Cyprus, Fuel oil No.6 is used for electricity generation. Table 4-2 gives the fuel properties and its composition. As it is mentioned in chapter 3, the combustion products are important as they are considered in the output exergy of the boiler. Table 4-3 shows the combustion products and the molar mass of each product in the flue gas coming out of the stuck at a velocity of 8 m/s. Equations 3-32, 3-33, 3-34, 3-35 and 3-36 are used to estimate the boiler irreversibilities and the exergy efficiency. As shown in Fig. 4-1, exergy efficiency is almost constant at 50% only slightly changing during the year, but the irreversibility rate has a linear relationship with the temperature and increase from 86 MW to 91 MW when the temperature rises from 17ºC to 37ºC (figure 4-2). In other words, for each degree centigrade rise in the temperature, the irreversibilities in boiler increase by 0.5 MW. This relation proves that heat transfer in a system has a noticeable effect on the exergy destruction rate.

Table 4-3. Properties of combustion products of Fuel oil No.6

Combustion products	Molar mass percentage	Standard chemical exergy $\bar{\varepsilon}^0$(kJ/kmol)
CO_2	47.28	20140
H_2O	38.41	1170
SO_2	0.6	303500
NO_2	0.7	56220
O_2	13	3970

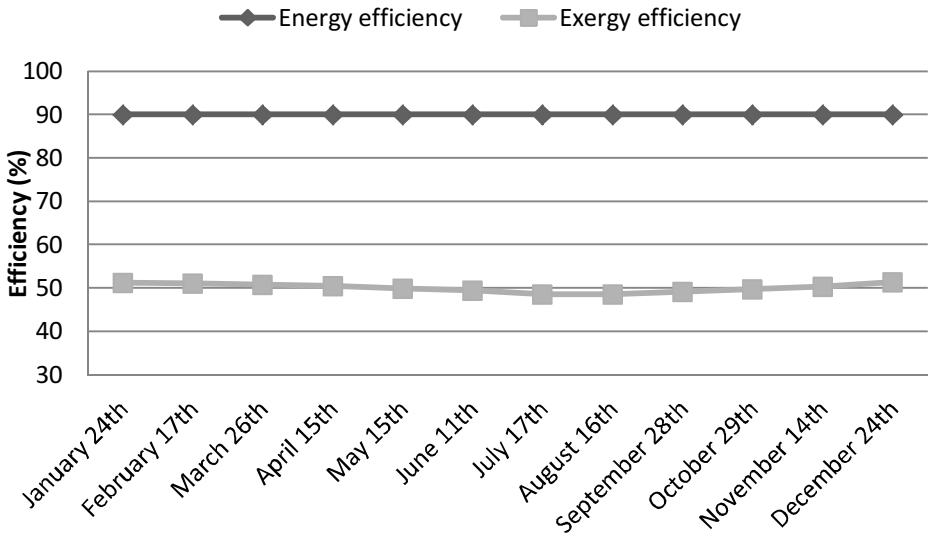

Figure 4-1. Energy and exergy efficiency of the boiler variation in different days throughout the year

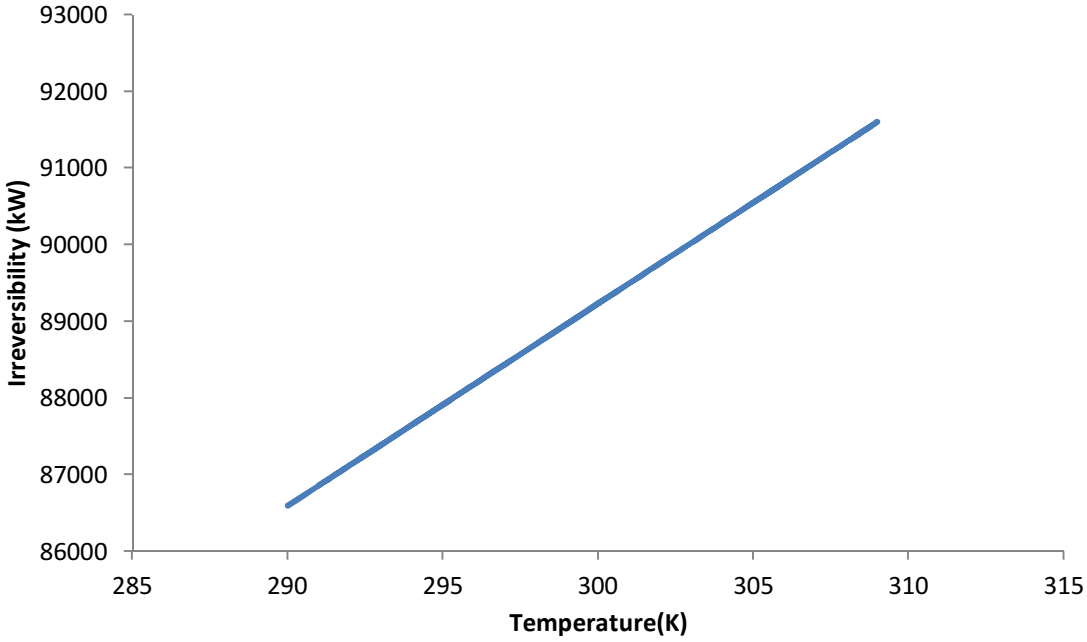

Figure 4-2. Variation of irreversibilities of the boiler with the ambient temperature

4.2.2 Turbine:

Table 4-4 shows the results of exergy and energy analysis of the turbine for specific days during year using equations 3-37 to 3-40.Energy efficiency is constant during the year since ambient temperature and quality of energy is not considered in energy analysis. Although exergy efficiency also does not vary considerably during the year, the irreversibility rate raises to 10118 kW in the hottest month of the year (Fig. 4-3). Generally, turbines have good exergy efficiency since the temperature of the output steam decreases extremely and the state of the output steam gets closer to the ambient temperature.

Table 4-4 Exergy analysis of the turbine for specific days of the weather data

Turbine					
Date	$\dot{E}x_{in}$**(kW)**	$\dot{E}x_{out}$**(kW)**	**Irreversibility(kW)**	η_I**(%)**	η_{II}**(%)**
January 24th	92303.8	22959.7	9863.1	62.7	85.8
February 17th	91899.2	22541.1	9877.1	62.7	85.8
March 26th	91090.7	21704.7	9905.0	62.7	85.7
April 15th	90284.8	20870.7	9933.1	62.7	85.7
May 15th	88686.2	19215.7	9989.5	62.7	85.6
June 11th	87499.7	17986.4	10032.2	62.7	85.6
July 17th	85140.5	15541.4	10118.1	62.7	85.5
August 16th	85140.5	15541.4	10118.1	62.7	85.5
September 28th	86707.6	17165.	10060.7	62.7	85.5
October 29th	88289	19225.9	9582.0	62.7	86.1
November 14th	89884.6	20456.4	9947.2	62.7	85.7
December 24th	92647.3	23318.9	9847.3	62.7	85.8

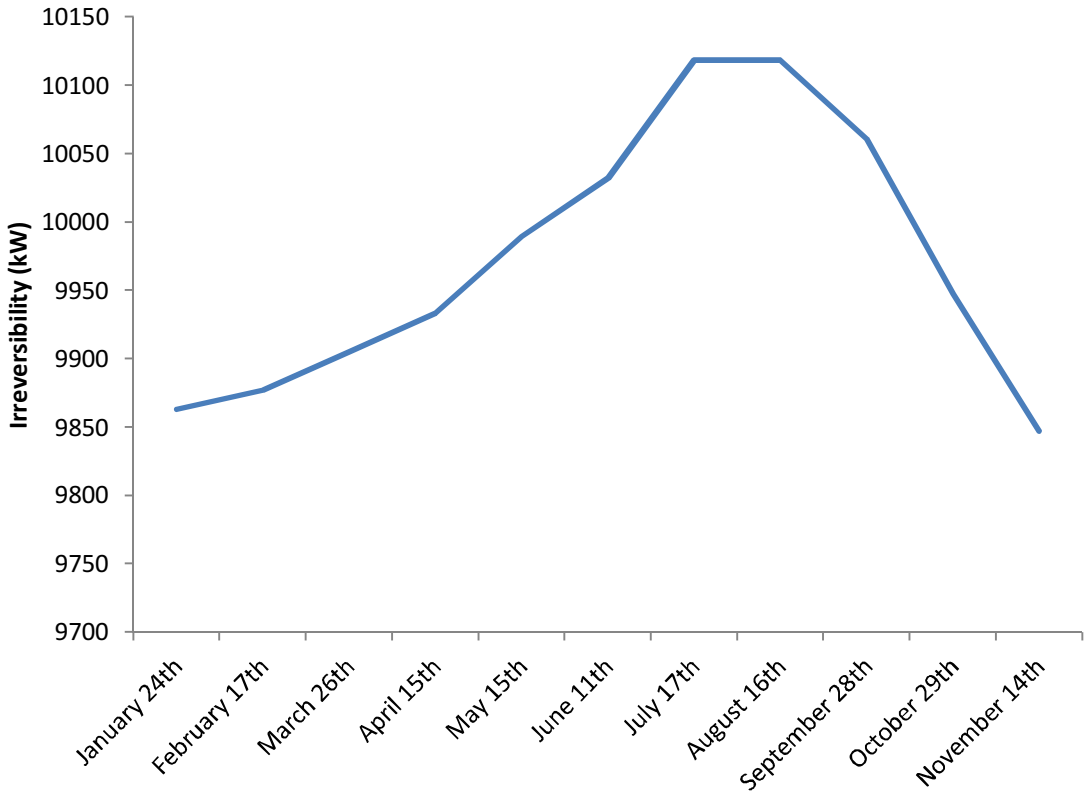

Figure 4-3. Variation of irreversibilities of the turbine throughout a year

4.2.3 Condenser:

In the condenser heat transfer takes place between the steam and the cooling water which is provided from the sea. Therefore, the irreversibilities (equation 3-4-43) increase with the temperature as shown in Fig. 4-4. Fig. 4-5 clearly demonstrates that the exergy efficiency which calculated by equation 3-44 decrease from 78% in January to its minimum in summer which is 4%. Since the condenser is related to the environment by the cooling water, the irreversibility rate does not have a very significant variation with the ambient temperature. Conversely, the ambient temperature has an excessive effect on exergy efficiency as a consequence of heat transfer and low exergy of the condenser output streams.

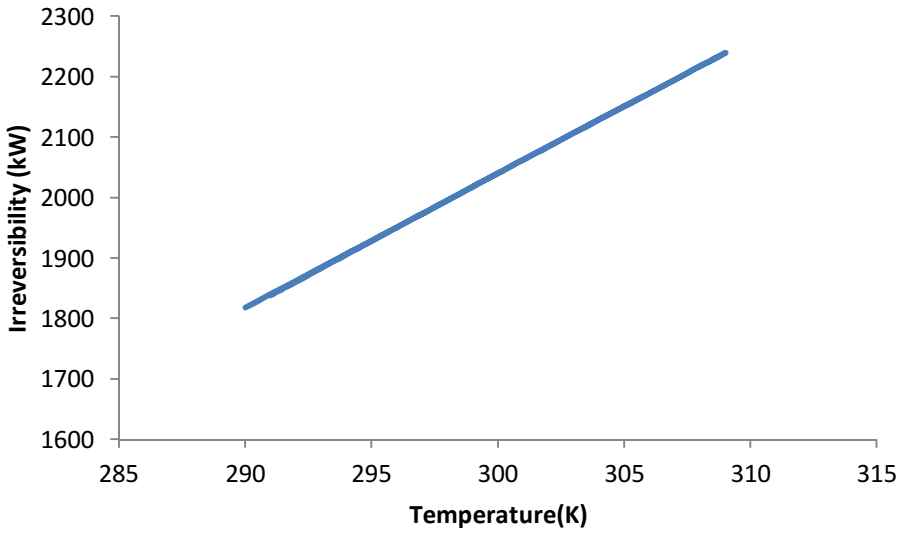

Figure 4-4. Variation of irreversibilities of the condenser with the ambient temperature

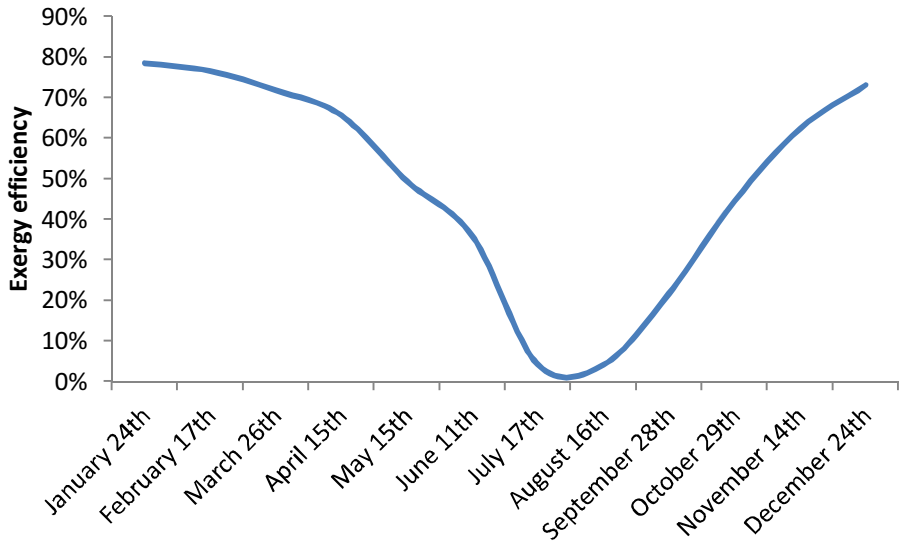

Figure 4-5. Variation of exergy efficiency of the condenser during a year

4.2.4 Pumps:

In the steam cycle two kinds of pumps are installed: condensate feedwater pump (CFP) and boiler feed water pump (BFP). CFP is pumping the output water with the flow rate of 44.996 kg/s of condenser to the first LP feed water heater with a pressure of 13 bars. The electrical and mechanical efficiency of this pump is 93.4% and 75.8% respectively and the work input is 179.63 kW. Boiler feed water pump which is placed after deaerator, pumps 53 kg/s of the water to the first HP heater with 105 bars. The output work of this pump is 1018.5 kW and it is working with electrical and mechanical efficiency of 95.7% and 75%, respectively. The exergy analysis of the pumps is carried out by using equations 3-45 and 3-46. Since BFP pumps a large mass of water with a high pressure, its irreversibilities are higher than CFP (Fig. 4-6), but also the exergy efficiency is more significantly more due to the higher exergy rate of the input stream (Fig. 4-7). The temperature does not affect the rate of irreversibility and exergy efficiency of the pumps since there is no heat transfer in the system. The rate of irreversibility rarely exceeds 450 kW which is not a high rate in comparison with boiler irreversibilities.

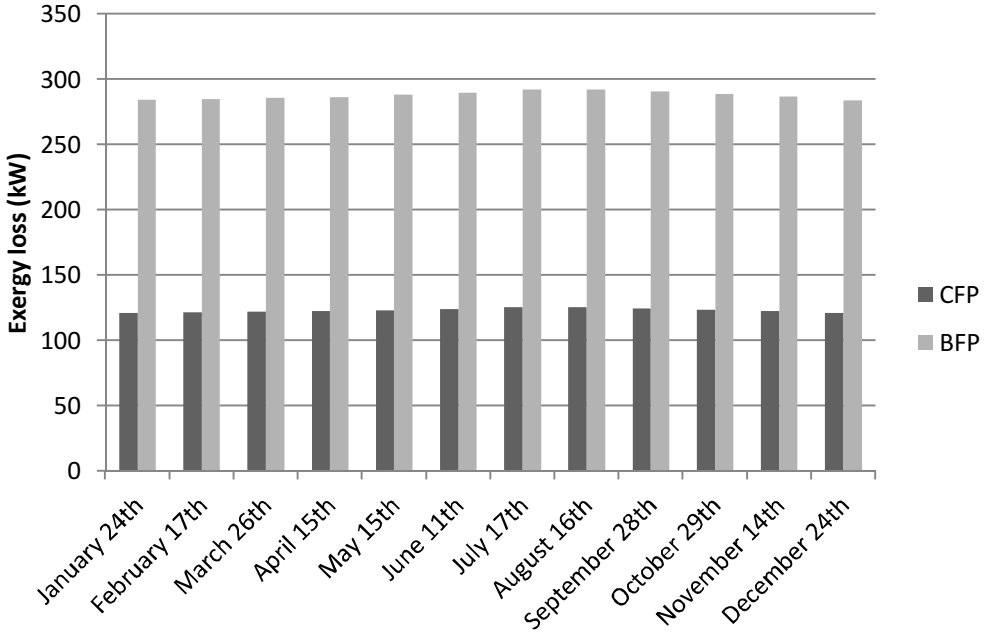

Figure 4-6. Variation of BFP and CFP exergy losses during a year

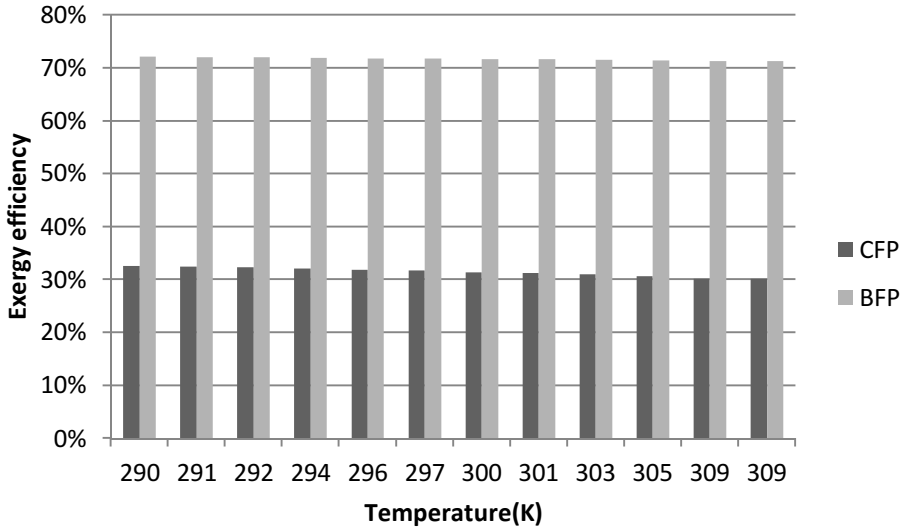

Figure 4-7. Variation of BFP and CFP exergy efficiency with the Ambient temperature

4.2.5 Feed Water Heaters:

Figure 4-8 shows the variation of the irreversibilities of the heaters in different months of a year. Except HP heater No.1 and deaerator, there is no significant change in exergy losses during a year for other feed water heaters. The source of the irreversibilities in the heaters is heat transfer between the steam extracted from the turbine and the water circulating in the cycle. LP heater No.1 and HP heater No.1 have the maximum and minimum exergy efficiency, respectively (figure 4-9). The exergy efficiency of the heaters does not vary significantly with temperature (equation 3-48).

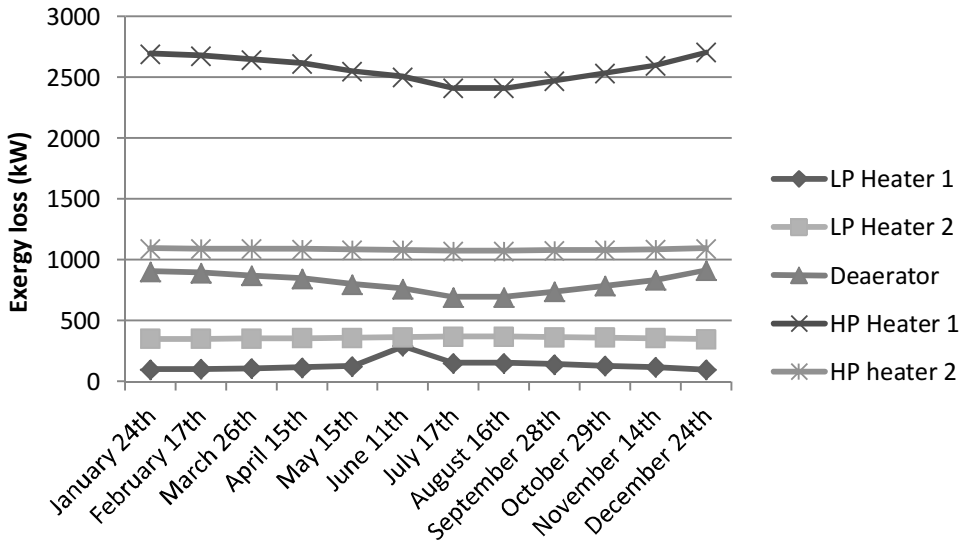

Figure 4-8. Variation of the exergy losses with the ambient temperature in feed water heaters

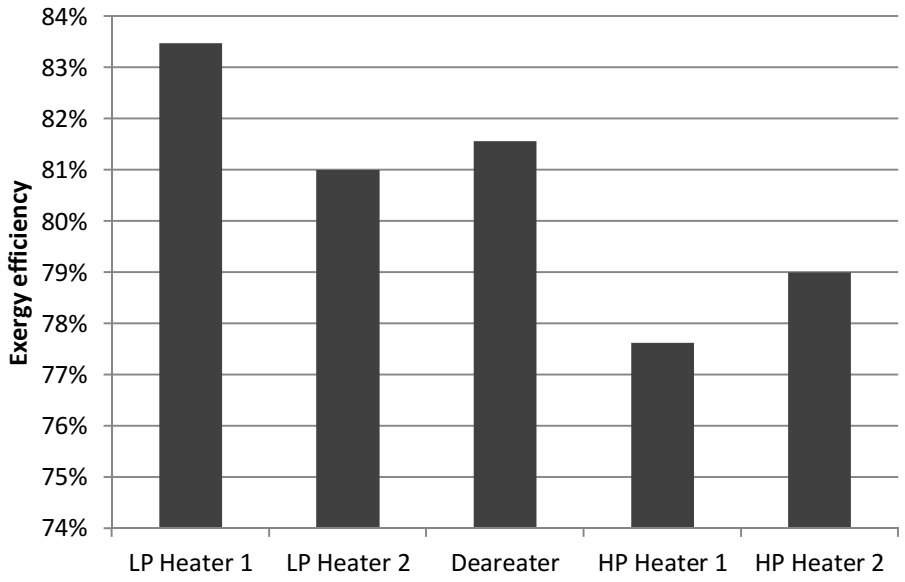

Figure 4-9. Comparison of the exergy efficiency in feed water heaters

4.2.6 Whole Power Plant:

The exergy efficiency of the steam power plant components is presented in Figure 4-10. Condenser and boiler have the lowest efficiency among the other components. The irreversibility rate of the whole plant is the sum of the irreversibilities of each component. As it has shown in Figure 4-11, boiler is the major exergy destructor due to the chemical reaction between air and fuel in the combustion process. Turbine is the second largest exergy consumer in the whole plant. While condenser operates with 49% of exergy efficiency, but Figure 4-12 reveals that only 2% of exergy loss happens there. Contrary to the second law analysis, this demonstrates that substituting the boiler system has more chances in enhancement of the overall efficiency of the plant.

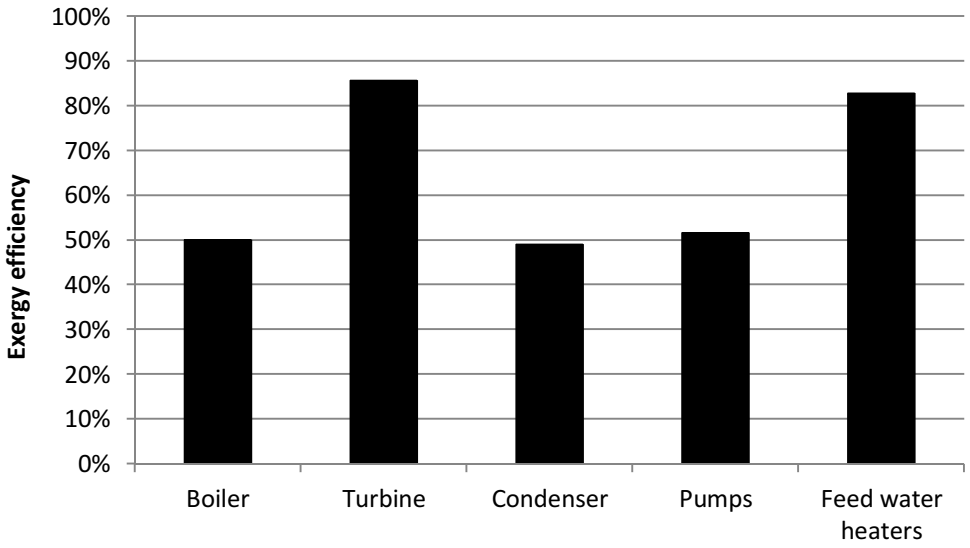

Figure 4-10. Comparison of exergy efficiency of the components of the steam power plant

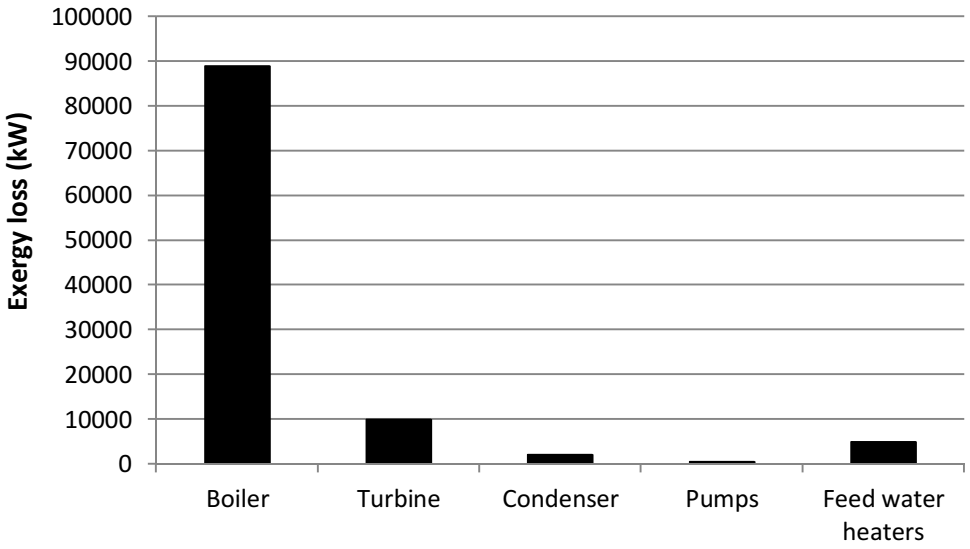

Figure 4-11. Comparison of exergy losses in the components of the 50 MW steam power plant

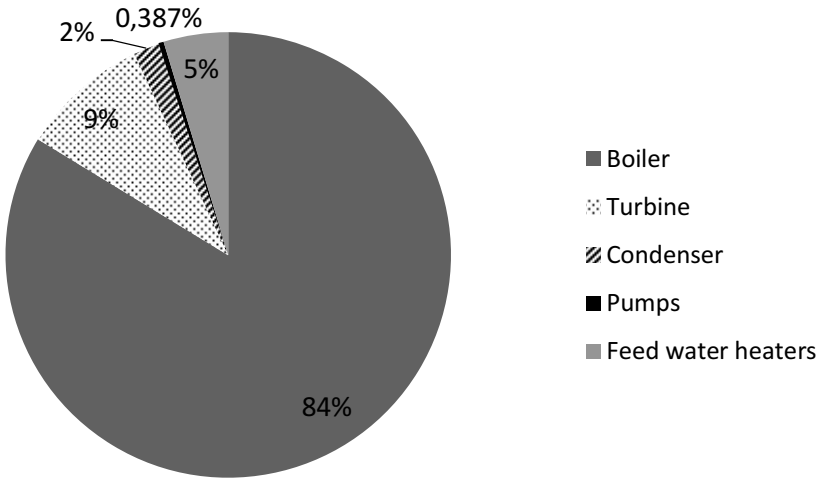

Figure 4-12. Percentage of irreversibility share of each component of 50 MW STPP

Chapter 5

ENERGETIC AND EXERGETIC ANALYSES OF 50 MW SOLAR THERMAL POWER PLANT

As it obtained from previous chapter, the major exergy destruction has been found in the boiler where 83% of the total exergy losses of the power plant cycle occurred as a result of combustion of the heavy fuel. Therefore, replacing the boiler with a system which produces steam without burning fossil fuels will be quite thought-provoking. Therefore, the solar thermal field is studied as an option for replacing the boiler.

5.1 System Description of 50 MW Solar Thermal Power plant

The 50MW STPP is designed based on direct steam generation (DSG). DSG technology avoids the use of a boiler in the power section since steam is directly generated in the solar field and the maximum temperature of the solar field coincides with the steam-cycle temperature.

In the present design, the solar collector field consists of 76 loops of ET-100 collectors and each row is composed of 10 collectors: 3 collectors for preheating water, 5 collectors for water evaporation and 2 collectors for superheating steam (Figure 5-1). The total collector field area is estimated 654480 m². The parameters of the ET-100 parabolic-trough collector and design-point parameters for the solar collector field are given in Table 5-1. The steam generated from solar collector field enters the turbine of the Rankine cycle at 510ºC and 87 bars. Location coordinates of Cyprus is 35.16° N and 33.35° E. The wind heat transfer coefficient is assumed to be

29 W/m².K. Figure 5-3 shows the average direct normal irradiation in the selected days in 2004 in Cyprus.

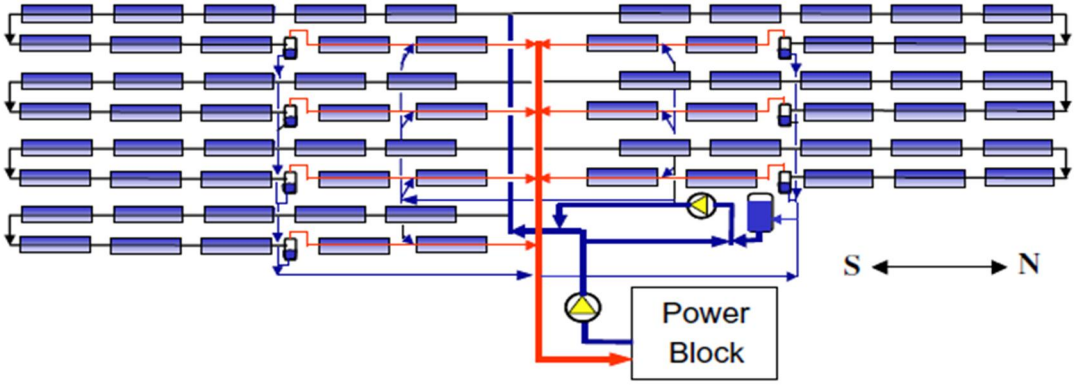

Figure 5-1. Simplified diagram of the DSG solar field [37]

Table 5-1. Design-point parameters of the ET-100 parabolic-trough collectors and their field arrangement [28].

Number of parabolic-trough modules per collector	12
Number of collectors in a row N_c	10
Number of collectors rows in collector field N_r	76
Gross length of every module	12.27 (m)
Aperture width B	5.76 (m)
Overall length of a single collector L	147.5 (m)
Inner/outer diameter of steel absorber pipe D_i/D_o	0.055/0.07 (m)
Inner/outer diameter of glass cover D_{ci}/D_{co}	0.125/0.130 (m)
Net collector aperture area per collector	848 (m^2)
Optical efficiency η_o at peak/design point	0.765/0.74
Intercept factor	0.92
Mirror reflectivity	0.92
Glass transmisitivity	0.945
Solar absortivity	0.94
Thermal emissivity	0.04795+0.0002331*T(°C)

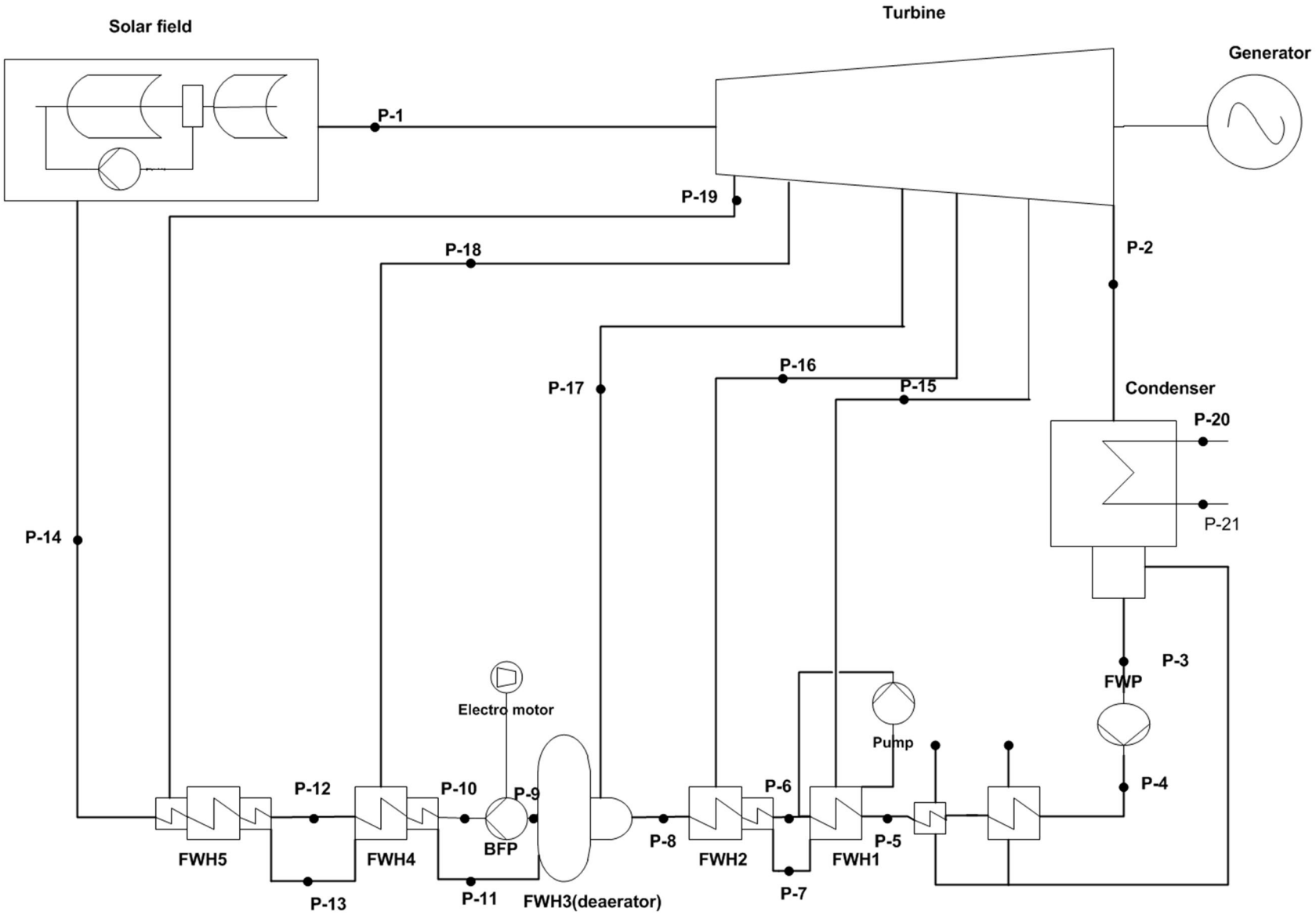

Figure 5- 2. Concentrating solar thermal power cycle

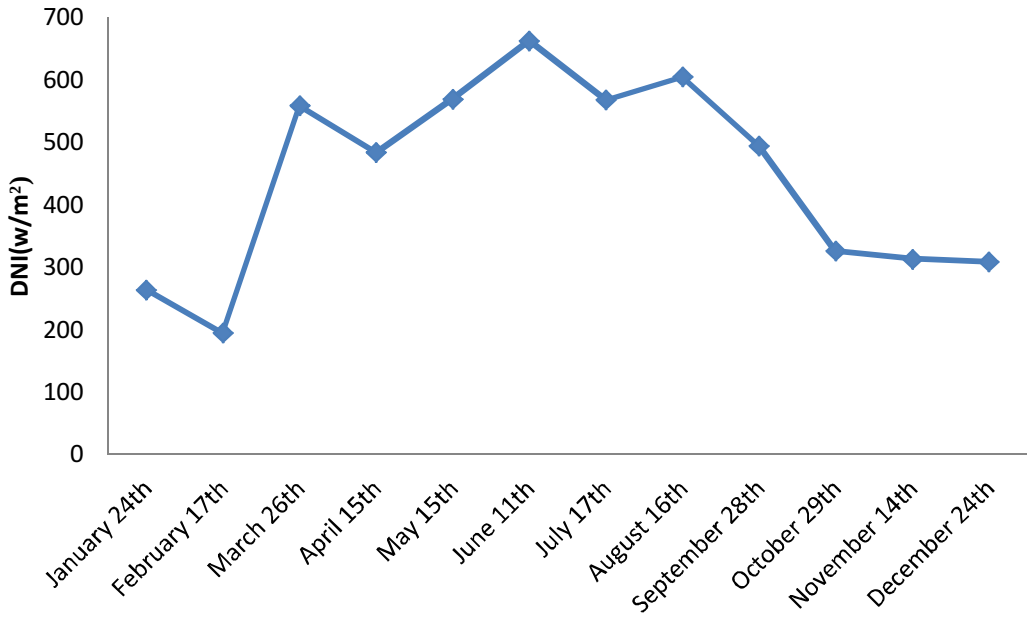

Figure 5-3. Average direct normal irradiation (DNI)

Table 5-2. Average ambient temperature and wind speed during a year for Cyprus

Month	Ta (°C)	Wind speed(km/h)
January	18	13.2
February	19	13
March	21	13.5
April	23	12.7
May	27	14.4
June	30	15.9
July	36	16.4
August	36	13.6
September	22	14.7
October	28	12.6
November	24	12.3
December	17	13.4

5.2 Energy and exergy analysis of the Solar Field:

As it mentioned in chapter 3, solar field has been divided into two subsystems: collector and receiver.

The heat loss coefficient $U_l = 1.4\ W/m^2K$ which is correlated with T_r ranging from 350 to 800 K is calculated by solving one dimensional model using EES software. This value is slightly lower than the true value since in the present study the conduction losses of some other components of the solar field, for instance receiver support brackets, is not considered.

Figure 5-4 has shown that, except the two first months of the year, the average energy losses of the receiver are higher than the collector subsystem. However, Figure 5-5 indicates that the exergy losses of the collectors are quite higher than the receivers. The solar field energy and exergy losses both occur their maximum and minimum values in June and February, respectively. Energetic and exergetic efficiencies of the solar field and the subsystems are shown in Fig. 5-6 and 5-7. It is assumed that the collectors absorb energy with a constant efficiency of η_o, therefore the collector energy and exergy efficiencies are almost constant throughout the year. The energy efficiency of the receiver is lower than the collector except for the two first months of the year. Unlike the energy efficiency, exergy efficiencies of the receivers are discernibly greater than that of the collectors for the first two and last three months of the year while it fluctuates around the 45% value during the rest of the year. The exergy performances are observed to take place in a different order as can be seen in Fig.5-7.

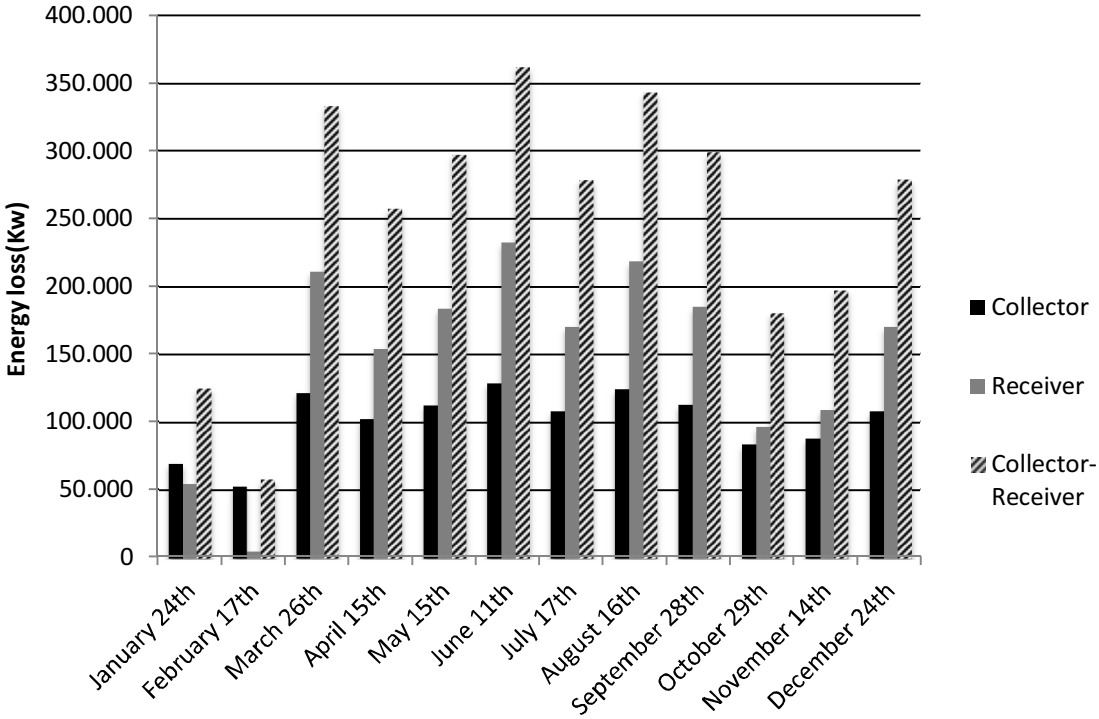

Figure 5-4. Average energy losses of the solar field

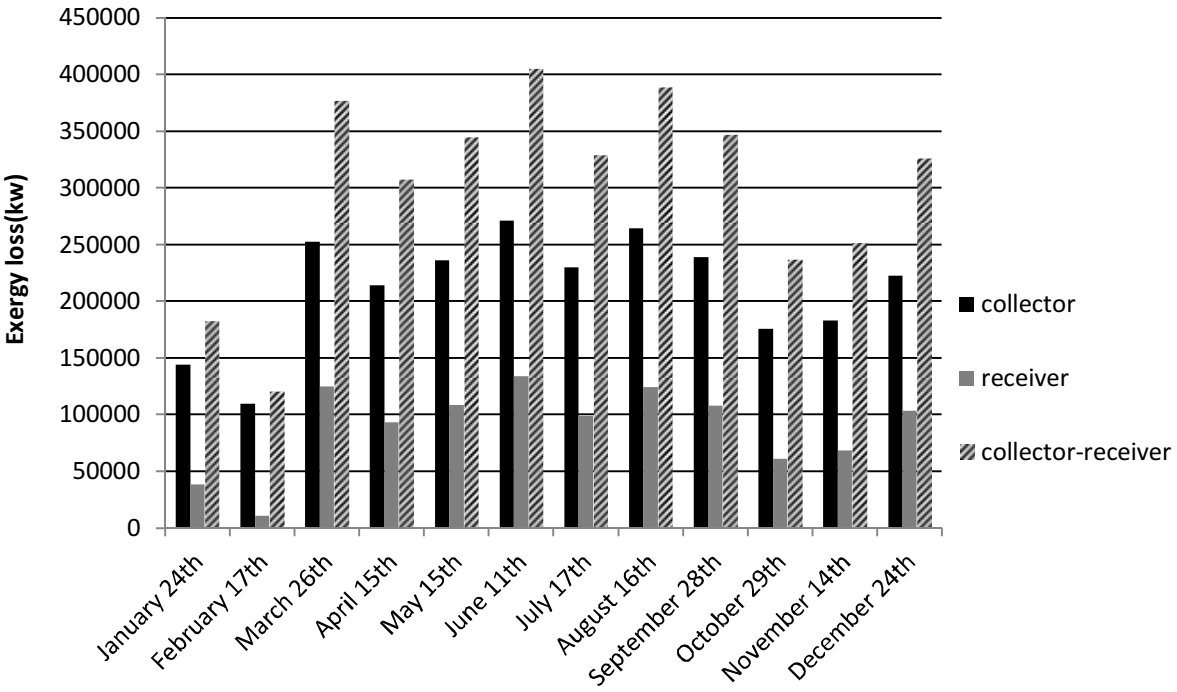

Figure 5-5. Average exergy losses of the solar field

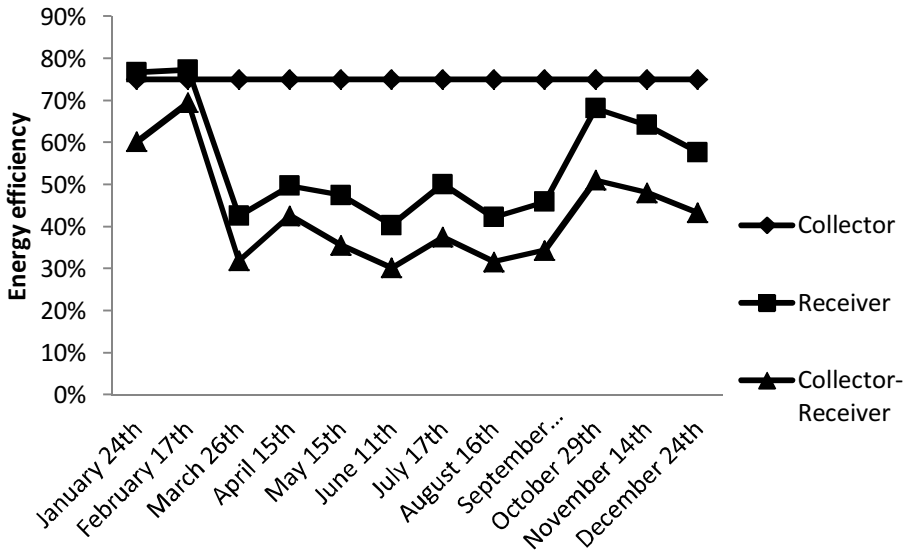

Figure 5-6. Energy efficiency of the solar field

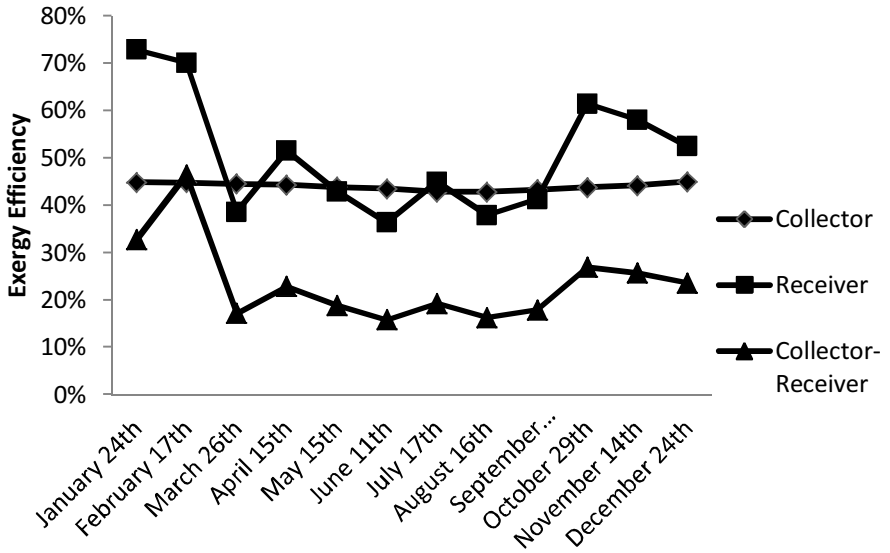

Figure 5-7. Exergy efficiency of the solar field

Exergy efficiency decrease from 46% to 15% while DNI increase from 194.03 to 662.26 W/m²K (figure 5-8). Therefore, the higher DNI results in higher losses and lower energy and exergy efficiency (figure 5-9). This fact explains that collector's capability in absorbing solar radiation besides transferring heat to the steam is poor. The solution of this deficiency can be found by studying and optimizing the design details of the solar field.

The changes in energy and exergy losses during a day are presented in Fig.5-10 and Fig.5-11, respectively. For the colder months which include January, October, November and December, it is observed that between 11 am to 2 pm the rate of losses drop since the DNI is increased. On the other hand, this value rises between the mentioned hours for the warmer months which are June, July and August. It is notable to mention that the energy and exergy losses have a direct relation with the rate of radiation which received by the solar field which is not just affected by DNI. As it is mentioned in Chapter 3, the radiation received by the solar field depends on the tilt factor and the declination δ which are the functions of $cos\theta, cos\theta_z$ and n.

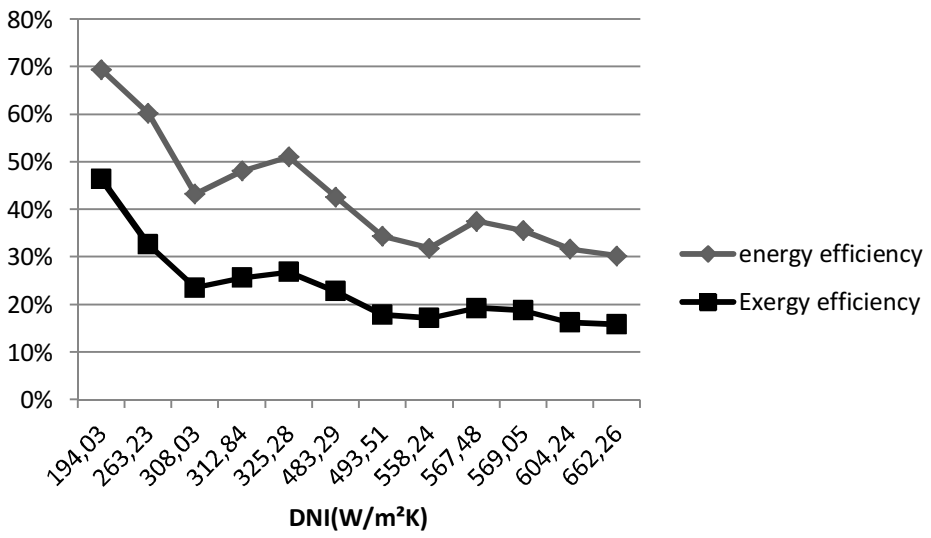

Figure 5-8. Variation of energy and exergy efficiency of the solar field with DNI

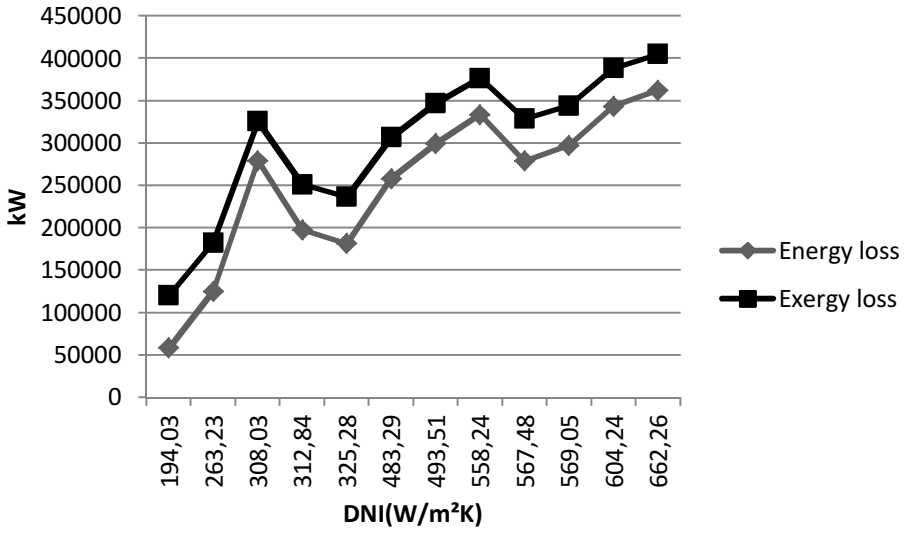

Figure 5-9. Variation of energy and exergy losses of the solar field with DNI

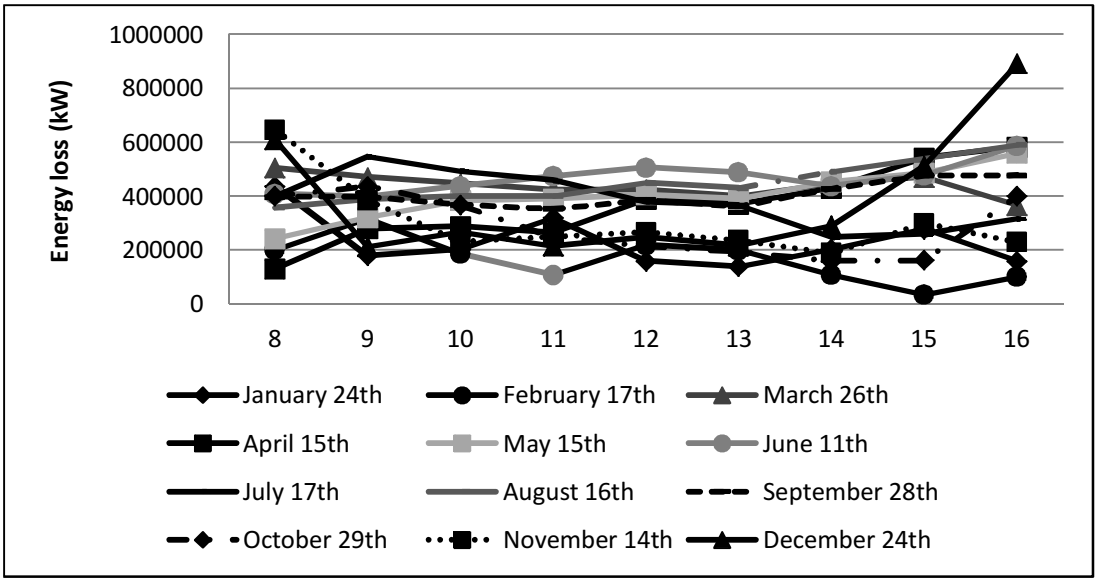

Figure 5-10. Variation of solar field energy losses for length of day throughout a year

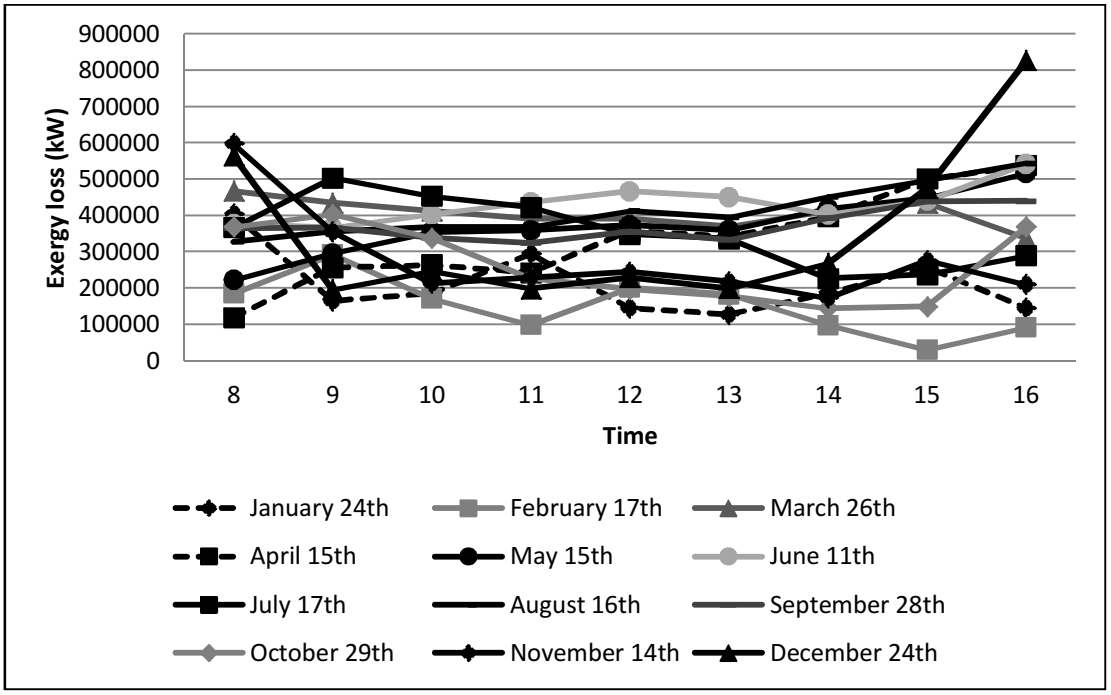

Figure 5-11. Variation of solar field exergy losses for length of day throughout a year

Chapter 6

DISCUSSION AND CONCLUSION

6.1 Discussion

The energetic and exergetic analysis has been carried out for the year round operation of existing steam power plant In Cyprus. In addition, the effects of ambient temperature on the exergy efficiency of the cycle and irreversibility rates have been studied.

It is found from the results that the main exergetic power loss takes place in the boiler followed by the condenser. Therefore, the main reasons of the irreversibilities are the combustion of the fossil fuel and the heat transfer processes. Moreover, the boiler irreversibility increases 0.5 MW per degree centigrade rise in the ambient temperature. Once the boiler is replaced by the solar field, the greater energy and exergetic power losses occur in the collector-receiver assembly. Unlike the energy losses, exergy losses of the collector are greater than that of the receiver. Furthermore, the energy and exergy efficiency of the STPP decrease while DNI rises due to the effect of incident angle. While the incident angle is related to the position and design parameters besides the tilt of the solar beam radiation, it demonstrates that significant improvement chances exist in the solar system rather than the boiler.

6.2 Comparison of the Results of STPP and Steam Power Plant:

Since a simple design of the solar field is considered, there is a high rate of the losses. Figure 6-1 compares the exergy efficiency of the solar field and the boiler. In contrast to the boiler, the rate of variation of exergy efficiency of the solar field during the year is very high. This fact improves an urge of an optimization in the solar field design and components. The maximum exergy efficiency of the solar field which is the closest to the boiler occurs in February with 47%. As it is shown in Fig. 5-3, the least DNI is received in February. Therefore the rate of heat transfers and hence the losses decrease.

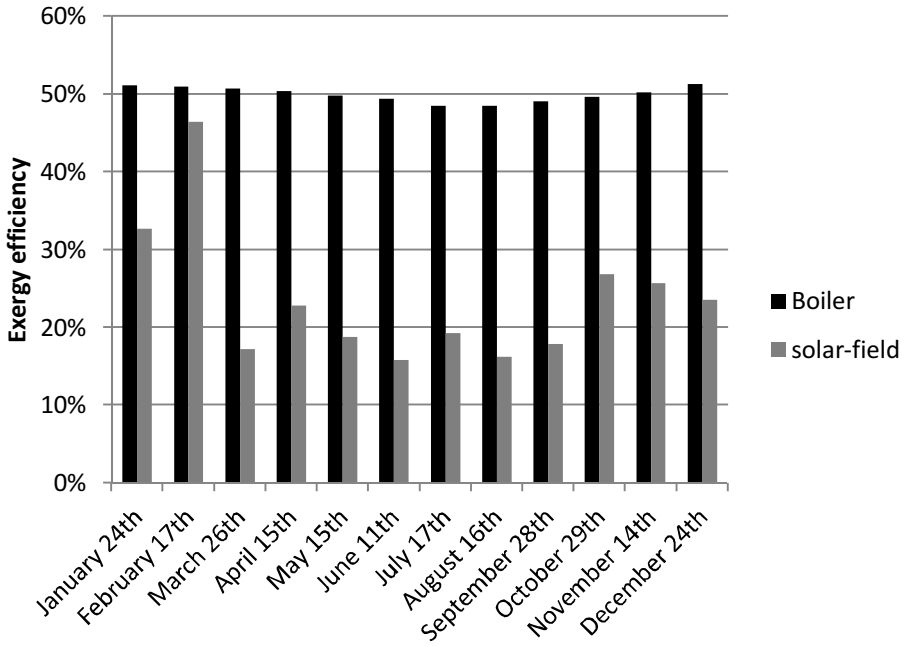

Figure 6-1. Solar- field exergy efficiency versus boiler exergy efficiency during one year

6.3 Suggestions for Optimization

Apparently, the solar collector-receiver assembly is the main area where the energetic and exergetic power losses are greatest. Following are several suggestions for optimizing the energy and exergy efficiency of the STPP conducting from results of this study:

- Collectors in the solar field have high energy losses. Increasing the number and changing the arrangement of collectors can improve the energy efficiency. To reduce exergy losses in collector, material constraints play an important role and hence, extensive work in this direction is to be carried out to make STPP a real success.
- Receivers have the most irreversibility due to the heat transfer. Therefore, changing the material or the length and diameter of the receiver tube can enhance the exergy efficiency of the receiver.
- Exergy of a system is carried out directly from the properties of the input and output stream flow of the system. Thus studying the effects of changing one or more properties e.g. pressure, will be effective. Moreover, the temperature of water at inlet to row of parabolic-trough collector must be optimum.
- Employing the boiler in the existing steam power plant as an auxiliary heater
- Increasing the temperature inlet water to the solar field by increasing the number of feed water heaters

REFERENCES

[1] Poullikkas A. (2009). Economic analysis of power generation from parabolic trough solar thermal plants for Mediterranean region-A case study for the island of Cyprus. *Renewable and Sustainable energy reviews 13*. 2474-2484

[2] http://www.cia.org.cy (Cyprus Institute of Energy).

[3] Hepbasli A. (2008). A key review on exergetic analysis and assessment of renewable energy resources for a sustainable future. *Renewable and Sustainable Energy Reviews 12.* 593-661.

[4] Goswami D.Y., Kreith F., Jan F. Kreidar J.F., 2000. Principles of Solar Engineering, second edition, Taylor and Francis.

[5] Quaschning V., Rainer K., Ortmanns W., (2002). Influence of direct normal Irradiance variation on the Optimal parabolic trough field size: a Problem Solved with Technical and Economical Simulations. *ASME Journal of Solar Energy Engineering*; 124-160.

[6] IEA Statistics and Balances retrieved (2011.05.08)

[7] Tzimas E. (2011). Sustainable or Not? Impacts and Uncertainties of Low-Carbon Energy Technologies on Water. AAS Annual Meeting 17–21 February, Washington DC.

[8] Renewables Global Status Report (2010). *REN 21*. 15.

[9] ACCIONA Website: Nevada Solar ONE project page. <http://www.acciona-na.com/About-Us/Our-Projects/U-S-/Nevada-Solar-One.aspx>

[10] Relloso, S., Delgado, E., (2009). Experience with molten salt thermal storage in a commercial parabolic trough plant. ANDASOL-1 commissioning and operation.

[11] Ishan Purohit , PallavPurohit. (2010). Techno-economic evaluation of concentrating solar power generation in India, *Energy Policy 38.* 3015–3029

[12] Eck, M., Zarza, E., (2002). Assessment of operation modes for direct solar steam generation in parabolic troughs. In: *Proceedings of the 11th Solar PACES International Symposium on Concentrated Solar Power and Chemical Energy Technologies*, Zurich, Switzerland. 591–598

[13] Zarza, E. Almerı´A. (2008). GDV: the first solar power plant with direct stem generation. In: *Proceedings of 14th International Solar PACES Symposium on Solar Thermal Concentrating Technologies*, Las Vegas, USA.

[14] Eck, M. (2008). Direct steam generation in parabolic troughs at 500.C .A. German–Spanish project targeted on component development and system design. In: *Proceedings of 14th International Solar PACES Symposium on Solar Thermal Concentrating Technologies*, Las Vegas, USA

[15] Kaushika S.C., Reddya V., Tyagib S.K, (2011). Energy and exergy analyses of thermal power plants: A review. *Renewable and Sustainable Energy Reviews 15*. 1857–1872

[16] Kotas Tj. (1985). The Exergy Method of Thermal Plant Analysis. Butterworths: London.

[17] Dincer I., Al-Muslim H., (2011). Thermodynamic analysis of reheats cycle steam power plants. *International Journal of Energy Research 25*. 727–739

[18] Fischer DW., (1996). Searching for steam system efficiency. *Plant Engineering 50*. 64–68.

[19] Ameri M., Ahmadi P., Khanmohammadi S., (2008). Exergy analysis of a 420MW combined cycle power plant. *International Journal of Energy Research 32*.175–183.

[20] Cihan A., Hac hafzoglu O., Kahveci K., (2006). Energy–exergy analysis and modernization suggestions for a combinedcycle power plant. *International Journal of Energy Research 30*.115-126.

[21] Habib M.A., Zubair S.M., (1992). Second-law-based thermodynamic analysis of regenerative-reheat Rankine cycle power plants. *Energy 17(3)*. 295-301.

[22] Rosen M., Tang R., (2006). Effect of altering combustion air flow on a steam power plant: energy and exergy analysis. *International Journal of Energy Research 31*. 219-231

[23] Singh N., Kaushik SC., (1994). Technology Assessment and Economic Evaluation of Solar Thermal Power Generation: A State of Art Report. IIT, Delhi.

[24] Singh N., (1994). Thermodynamic and technoeconomic assessment of solar thermal power generation. *Ph.D. thesis*, CES, IIT, Delhi.

[25] Bannister P., (1998). A basic model of a high temperature solar thermal power collector system. In: *Proceedings of the Annual Conference of the Australian and New Zealand Solar Energy Society*, University of Melbourne, 17-19 November.

[26] Bannister P., (1998). Exergy and solar thermal power generation. In: *Proceedings of the Annual Conference of the Australian and New Zealand Solar Energy Society,* University of Melbourne, 17-19 November.

[27] Singha N., Kaushikb S.C., Misrac R.D., (2009). Exergetic analysis of a solar thermal power system. *Renewable Energy 19*.135-143.

[28] Gupta M.K., Kaushik S.C., (2010). Exergyanalysis and investigation for various feed water heaters of direct steam generation solar–thermal power plant, *Renewable Energy 35*. 1228–1235.

[29] Dincer I., (2002). On energetic, exergetic and environmental aspects of drying systems. *International Journal of Energy Research 26*.717–27.

[30] Duffie John A., Beckman William A., (1991). Solar engineering of thermal processes. Second edition. New York: John Wiley and Sons, Inc.

[31] Lupfert E., Geyer M., Schiel W., Esteban A., Osuna R., Zarza E., Nava P., (2001). EUROTROUGH design issues and prototype testing at PSA.In: *Proceeding of ASME international solar energy conference-forum, solar energy: the power to choose*, Washington, DC; April 21-25. 389-394.

[32] Price H., Eckhard L.P., David K., Zarza E., Gilbert C., Randy G. (2002). Advances in parabolic trough solar power Technology. *Journal of Solar Energy Engineering 25*.124-109.

[33] Xu C., Wang Z., Li X., Sun F., (2011). Energy and exergy analysis of solar power tower plants. *Applied Thermal Engineering 31*. 390-413

[34] Odeh S.D., Morrison G.L., Behnia M., (1998). Modeling of parabolic trough direct steam generation solar collectors. *Journal of Solar Energy 62*. 395–406

[35] Kotas T.J. (1985). The Exergy Method of Thermal Plant Analysis. Butterworths: London.

[36] Cengel Y.A., Boles M.A., (2007). Thermodynamics: An engineering approach, 6th edition, McGraw-Hill.

[37] Zarza. A., Esther Rojas M., Gonza´lez L., Caballero J.M., Rueda F., (2006). INDITEP: The first pre-commercial DSG solar power plant. *Journal ofSolar Energy 80* . 1270–1276

[38] Siva Reddy V., Kaushik S.C., Tyagi S.K.. (2010). Exergetic analysis and performance evaluation of parabolic trough concentrating solar thermal power plant (PTCSTPP). *Journal of Energy 39* .258-273

[39] Montes M.J., Aba´nades A., Martı´nez-Val J.M., (2009). Performance of a direct steam generation solar thermal power plant for electricity production as a function of the solar multiple. *Journal of Solar Energy 83*. 679–689

[40] Ameri M., Ahmadi P., Hamidi A., (2008). Energy, exergy and exergoeconomic analysis of a steam power plant: A case study. *International Journal of Energy Research 33.* 499-512.